

AD-A020817



NORWAY

DDESB Library Copy

add

# FORTIFIKATORISK

NOTAT NR<sup>103</sup> / 75

Airblast Propagation Through Tunnels  
and the Effects of Wall Roughness

APR 1975

BEST AVAILABLE COPY

FORSVARETS BYGNINGSTJENESTE

ADA020817

NORWEGIAN DEFENCE CONSTRUCTION SERVICE  
Office of Test and Development

Fortifikatorisk notat nr 103/75

Airblast Propagation Through Tunnels  
and the Effects of Wall Roughness

by

A.T. Skjeltnorp

April 1975

## TABLE OF CONTENTS

	Page
ABSTRACT	1
1. INTRODUCTION	2
1.1 Background	2
1.2 Objectives	2
1.3 Scope	2
2. THEORETICAL CONSIDERATIONS	3
2.1 Blast Wave Formation in Tunnels	4
2.2 Diffraction Region	4
2.3 Build-up Region	5
2.4 Turbulent Choke	5
2.5 Shock-Front Attenuation due to Wall Roughness	5
2.6 Shock-Front Attenuation due to Rarefaction Waves	10
3. EXPERIMENTAL RESULTS AND DISCUSSION	12
3.1 Large Scale Tests in Tunnels	12
3.2 Tests in a 0,05 m Diameter Tube	14
3.3 Analysis of Test Results in Tunnels	15
4. EFFECTS OF TUNNEL ROUGHNESS ON EXTERNAL SAFETY DISTANCES	17
5. CONCLUSIONS	19

## REFERENCES

Table 4a

Figures

## A B S T R A C T

This report reviews the possibility of large airblast attenuation in the case of rough-walled tunnel systems in underground ammunition storage sites. A comparison is made between the peak pressure attenuation observed in three tests with tunnel diameters ranging from 2,7 - 6 m. These results are shown to be consistent with a semi-empirical theory for steady turbulent flow in rough tunnels.

The use of tunnels with large wall roughness is shown to reduce considerably the hazardous area around an underground ammunition storage site compared to sites with smooth-walled tunnels.



## 1. INTRODUCTION

### 1.1 Background

This report originated in connection with the analysis of a large scale test called "Operation Block" /1, 2/ concerning safety aspects of underground ammunition storage. One part of this test was to measure the blast at various distances along the main passageway leading into the storage chamber. These results showed such a high shock front attenuation compared to the results from model tests /3, 4/ that it initially caused a suspicion that there had been erroneous readings from the pressure gauges. However, subsequent analysis showed that the results were qualitatively consistent with the large difference in wall roughness between the prototype and the model /3, 4/.

### 1.2 Objectives

The basic objective of this report is to show that the large airblast attenuation observed in the "Operation Block" test, is in fact comparable to the results from various other large scale tests with similar wall roughness. These data are thus of considerable interest as there are strong indications that the hazardous area around an underground ammunition storage site will be reduced considerably if the tunnel walls have a large roughness.

### 1.3 Scope

In Sec. 2, a phenomenological description of airblast in tunnels is given and a semi-empirical theory for steady turbulent flow in rough tunnels is reviewed. This will be compared with experimental findings in Sec.3. The effects of tunnel roughness on external safety distances in underground ammunition storage sites will be discussed in Sec.4 and the principal results are finally summarized in Sec.5.

## 2. THEORETICAL CONSIDERATIONS

A great deal of attention has been directed in recent years to the subject of shock front attenuation due to wall roughness as evidenced by the experimental and theoretical work reviewed in Ref.5. For the most part, these tests have been performed in relatively smooth-walled tubes (shock tubes) of moderate diameters (order of centimeters). There are, however, various data on air-blast in rock-tunnels of relatively large diameters (order of meters) with considerable wall roughness. These data are therefore of interest in connection with underground ammunition storage.

Before specific examples are discussed, a brief review will be given of some of the effects influencing the blast wave propagation in straight tunnels such as:

- a) The friction between the moving air and the tunnel wall.
- b) The pressure gradients in the wave behind the shock front (rarefaction waves) which continuously degrades the front.
- c) Thermal energy transmission to the walls (conduction/convection and radiation).
- d) Elastic or inelastic deformation of the walls.

For rough-walled rock tunnels, the blast wave attenuation is dominated by a). For peaked wave forms the effect in b) will also be of some importance. The effects in c) and d) are expected to be comparably unimportant as discussed elsewhere /6/.

In the following sections, various aspects of the initial blast wave formation in tunnels will be discussed followed by a discussion of the effects from a), assuming a relatively flat pressure wave. In this case the effect in b) can be neglected, and will be discussed separately in Sec. 2.6.



## 2.1 Blast Wave Formation in Tunnels

Before a steady state one-dimensional blast wave propagation in tunnels takes place, there are various initial blast wave diffraction patterns characteristic for the specific geometries in question. Typical examples are shown schematically in Fig. 2.1 with:

- a) Detonation of a charge in a straight tunnel.
- b) Shock wave entering a tunnel.
- c) Detonation of a charge in a chamber adjacent to the tunnel.

Cases a) and c) are of particular interest for underground ammunition storage, whereas case b) is of interest in underground protective installations.

Porzel /7/ has given a phenomenological description of case b) in Fig. 2.1 with a surface wave entering a tunnel and suggested that the subsequent blast wave propagation down a rough-walled tunnel is characterized by five mechanisms:

Diffraction, buildup, turbulent choke, wall friction and feedback.

Although the situation is somewhat different for cases like a) and c) relevant for underground ammunition storage, this model description will give some insight into the basic phenomena and will therefore be reviewed briefly in the following sections.

## 2.2 Diffraction Region

The initial blast wave propagation in the tunnel is characterized by complicated diffraction patterns. It is therefore not readily possible to define a unique diffracted pressure  $p_D$ . For engineering use it is at best possible to define  $p_D$  as an average pressure in space and time.

### 2.3 Build-up Region

After a few tunnel diameters  $(L/D)_B$ , say, there is a pressure build-up due to the succession of reflected pressure waves off the tunnel walls with the formation of a Mach stem. Again, it is hardly possible to define a build-up pressure  $p_B$  at a specific distance  $(L/D)_B$ . For engineering use  $p_B$  can approximately be thought of as being the average pressure of more or less definite shocks which coalesce at a few tunnel diameters downstream from the diffraction region. For example, for case b) in Fig. 2.1 with a surface wave entering a tunnel, empirical fits to various measurements have tentatively produced  $p_B \simeq (1,4 \pm 0,2) p_D / 7/$ .

To calculate these types of diffraction patterns from first principles for a real three-dimensional case, appear to be prohibitively difficult. It is therefore usually necessary to rely on previous experiments or specific model tests in each particular case.

### 2.4 Turbulent Choke

After the formation of the more or less definite Mach stem described in Sec. 2.3, the wall roughness produces turbulent boundary layers which steadily grow out from the wall. Soon the boundary layers will converge at a certain distance behind the shock as indicated in Fig. 2.4. At the center of this closure the material flow will be stagnated. This situation is referred to as a turbulent choke. Assuming a steady-state situation with a constant distance for choke formation behind the shock and isentropic flow behind the shock, the model relates the "choked" overpressure  $p_C$  at the front to the buildup overpressure  $p_B$  as

$$p_B = (1 + p_C) \left[ 1 + \frac{5p_C^2}{7(1 + p_C)(7 + p_C)} \right]^{7/2} - 1 \quad (2.4)$$

with pressures expressed in bars.

### 2.5 Shock-Front Attenuation due to Wall Roughness

An example of a shock wave passing over an idealized



roughness element is shown in Fig. 2.5a. Clearly, in a naturally excavated tunnel with large wall projections at random, there will be a very complex pattern of shock reflections which will drastically affect the shock front. Detailed calculations of the blast wave propagation from first principles will obviously be prohibitively difficult.

It is beyond the scope of this report to give a critical review of the many approximate models dealing with this problem /5/. A so called shock impedance model originally proposed by Porzel /7/ is conceptually simple and appear to reproduce various experimental results of the present type reasonably well and will be discussed next.

The basic assumption for this model can be expressed as follows:

The loss in the shock energy due to wall roughness is proportional to:

- a) The kinetic energy per unit volume at the shock front,  $E_{k,v}$ .
- b) The volume subtended by the average wall roughness of the tunnel walls or  $\bar{e} \cdot S \cdot dL$ , where  $\bar{e}$  = average height of the projections,  $S$  = perimeter of the tunnel, and  $dL$  = distance traversed by the shock.
- c) An efficiency factor  $\epsilon$  postulated to be in the range  $1/2 \leq \epsilon \leq 1$ .

The infinitesimal loss in total energy over a distance  $dL$  can therefore be expressed as

$$dE = -\epsilon \cdot E_{k,v} \cdot S \cdot \bar{e} \cdot dL. \quad (2.5a)$$

Letting  $dE_{t,v}$  represent the total energy per unit volume, i.e.  $dE = A \cdot D \cdot dE_{t,v}$ , Eq (2.5a) can be expressed as

$$dE_{t,v}/E_{k,v} = -4 \epsilon (\bar{e}/D) d(L/D) \quad (2.5b)$$

Here,  $D$  designates the hydraulic diameter defined by

$$D = \frac{4A}{S} \quad (2.5c)$$

with  $A$  = cross-sectional area and  $S$  the perimeter of the tunnel.

Eq (2.5b) as it stands is of course not very convenient for practical use, but can be re-expressed in terms of the front pressure using the usual Rankine-Hugoniot equations. This produces an equation of form:

$$Y(p) = \text{constant} - 2 \epsilon (\bar{e}/D)(L/D) \quad (2.5d)$$

where  $Y(p)$  is an impedance function defined as

$$Y(p) = \frac{2\mu + 1}{\mu + 1} \ln p - \frac{\mu}{\mu + 1} \ln(p + \mu + 1) - \frac{1}{p} \quad (2.5e)$$

Here,  $p$  is the dimensionless overpressure ratio

$p = p_{so}/p_o$  with  $p_{so}$  = static overpressure and

$p_o$  = ambient pressure.

Expressing  $p_{so}$  in bars and using  $p_o = 1$  bar, we have nominally  $p = p_{so}$ . We will therefore in the remainder of this report not distinguish between  $p$  and  $p_{so}$ .

Furthermore,  $\mu$  is a thermodynamic parameter

$$\mu = (\gamma + 1)/(\gamma - 1) \quad (2.5f)$$

where  $\gamma$  is the usual ratio of the specific heats,

$\gamma = C_p/C_v$ . For air under standard conditions  $\gamma = 1.4$

which gives  $\mu = 6$  and Eq (2.5e) takes the simpler form

$$Y(p) = \frac{13}{7} \ln p - \frac{6}{7} \ln(p + 7) - \frac{1}{p} \quad (2.5g)$$

This function is shown in Fig 2.5b.

It is interesting to note that in the high pressure limit,  $p \gg 7$ , Eq (2.5g) reduces to  $Y(p) = \ln p$  and therefore  $\ln p = \text{constant} - 2\epsilon \frac{\bar{e}}{D}$ ,

which has the solution:

$$p_2 = p_1 \exp \left( -k \frac{L_2 - L_1}{D} \right), \quad (2.5h)$$

with an attenuation constant

$$k = 2\epsilon \frac{\bar{e}}{D} \quad (2.5i)$$

Eq (2.5h) is the form for the blast wave attenuation originally proposed by Emerich and Curtis in Ref.8. This equation was also used by this office in an earlier analysis of blast wave propagation in tubes and tunnels /9/.

Eq (2.5d) is in a form which allows the determination of pressure attenuation due to a given relative roughness  $\bar{e}/D$ . The length of tunnel required to reduce the pressure from  $p_1$  to  $p_2$  can thus be found from

$$Y(p_1) = \text{constant} - 2\epsilon \frac{\bar{e}}{D} \frac{L_1}{D} \quad (2.5j)$$

$$Y(p_2) = \text{constant} - 2\epsilon \frac{\bar{e}}{D} \frac{L_2}{D} \quad (2.5k)$$

$$Y(p_1) - Y(p_2) = 2\epsilon \frac{\bar{e}}{D} \left( \frac{L_2}{D} - \frac{L_1}{D} \right) \quad (2.5l)$$

This shows that there ought to be a linear relationship between the impedance function  $Y$  and the distance  $L$  in the tunnel.

The definitions of  $\bar{e}$  and  $\epsilon$  need further clarifications. For very irregular tunnel walls, the determination of  $\bar{e}$  will obviously be quite uncertain. This is of course not only the case for this



particular model, but for any model attempting to describe wall roughness attenuation. For engineering use, an adequate value can be loosely expressed as

$$\bar{e} = \int e d(\text{Area}) / \int d(\text{Area}), \quad (2.5m)$$

where  $e$  equals the depth of the roughness elements and the area is integrated over the wall of the tunnel.

Examples of idealized wall roughness elements are shown in Fig. 2.5c and estimates of  $\bar{e}$  using Eq (2.5m) are given. For a tunnel blasted out of rock, a reasonable value for  $\bar{e}$  appears to be

$$\bar{e} \approx \frac{1}{2} e_{\max},$$

where  $e_{\max}$  is the maximum height of the roughness elements. Clearly, only experiments will be able to clarify the adequateness of this definition of  $\bar{e}$ . This will be discussed in Sec. 3.

The constant  $\epsilon$  in Eq (2.5d) is related to the amount of kinetic energy stagnated within the volume extended by the roughness. It has been postulated that  $\epsilon = 1$  in the early period of the shock propagation of the tunnel, i.e. all the kinetic energy is stagnated and not immediately available for supporting the shock ("strong impedance"). At later times, approximately 50% of this stagnated energy becomes hydrodynamically available to be propagated in the forward direction toward the shock front.

This is therefore a "feedback" situation and one has approximately  $\epsilon = \frac{1}{2}$  ("weak impedance"). Earlier tests have indicated that there is a more or less definite distance at which point  $\epsilon$  changes its value from 1 to  $\frac{1}{2}$ . Empirically, this "feedback" distance



has been determined to be approximately given by:

$$(L/D)_F \approx 18/(\epsilon \frac{\bar{e}}{D})^{0,3} \quad (2.5n)$$

For an effective roughness factor  $0,05 < \bar{e}/D < 0,1$ , the corresponding feedback distance is  $44 > (L/D)_F > 36$ .

## 2.6 Shock-Front Attenuation due to Rarefaction Waves

In the discussion of the blast wave propagation in the previous sections, the input was assumed to be relatively constant in time. A characteristic feature of the propagation of a peaked blast wave along a tunnel is that the higher pressure regions toward its front move at higher velocities than the shock front and lower pressure regions. The shock front is thus overtaken by the lower pressures of the rarefaction wave, which causes an attenuation of the shock front. At the same time this also results in an increase in the positive duration or wavelength with travel distance. This is illustrated in Fig. 2.6a.

Various simplified models have been proposed to characterize this phenomenon /5/, but one of the most rigorous descriptions has probably been presented by Porzel /7/ with the following result for the infinitesimal shock front attenuation with distance:

$$\frac{dp}{dL} = f(p) \frac{1}{u} \frac{\partial p}{\partial t} \quad (2.6a)$$

Here,  $f(p)$  is a relatively complicated function of the front pressure  $p$  and  $u$  is the shock front velocity.  $\partial p / \partial t$  is the slope of the rarefaction wave at the front as indicated in Fig 2.6a. Clearly, for a flat shock front, as is approximately the case in an ordinary air-driven shock tube,  $\partial p / \partial t = 0$  and there is no front pressure reduction due to this effect.

The use of Eq (2.6a) for peaked shock waves presumes a knowledge of the initial pressure-time history at some position in the tunnel. In practice, for underground ammunition storage,  $\partial p / \partial t$  cannot easily be defined. A purely empirical approach based on model tests, has therefore been used to establish the "smooth wall" pressure-distance relationships for various explosive weights in a relatively wide range of tunnel systems shown in Fig 2.6b /10-12/:

$$p = f(a_1, a_2, \dots)(Q/V_t)^{C_2} \quad (2.6b)$$

Here,  $Q$  is the explosive charge (TNT) and  $V_t$  the total volume traversed by the blast wave up to the observation point as indicated in Fig 2.6b.  $f(a_1, a_2, \dots)$  in Eq (2.6b) is a function depending on the exact geometry around the area of detonation with  $a_1, a_2, \dots$  indicating geometrical parameters such as cross-sectional areas, angles etc. The exponent  $C_2$  is found to be remarkably reproducible for the various configurations with  $C_2 = 0,6 \pm 0,1$ .

Eq (2.6b) shows therefore that for a given configuration the pressure varies roughly as

$$p \propto (Q/V_t)^{0,6 \pm 0,1} \quad (2.6c)$$

These observations will be used later in Sec 3 in the analysis of blast wave attenuation in rough-walled tunnels.

It is interesting to compare the pressure dependence for various confinements. In Fig 2.6c the results for TNT detonations in free air /14/ in a tunnel /10/, and in a closed chamber /13/ are shown. Here, the average peak pressures are given versus an effective loading density  $Q/V$ , where  $Q$  is the TNT charge weight and  $V$  the total volume traversed by the blast wave up to the observation point. As may be seen, the results differ remarkably little in the pressure



range 5 - 100 bar corresponding to effective loading densities ranging from 0,1 to 10 kg/m<sup>3</sup>. In fact, the differences are less than about 30%. For higher and lower loading densities the differences are becoming significant. It is also interesting to note that the tunnel data on the average appear to lay roughly between the free air and closed chamber data. This is reasonable on physical grounds because TNT is deficient in oxygen and the detonation energy is dependant on the confinement.

### 3. EXPERIMENTAL RESULTS AND DISCUSSION

#### 3.1 Large Scale Tests in Tunnels

A full scale test called "Operation Block" was conducted in 1973 by the Royal Swedish Fortification Administration /1, 2/. The basic objective of this test was to study the possibility of reducing the hazardous area outside an underground ammunition storage by installing a moveable concrete block in the branch passageway. In conjunction with the full scale test, a series of model tests in a linear scale 1:50 were performed in Norway /3, 4/. In particular, one part of the tests was to measure the pressure-time history in the branch- and main passageway leading into the storage chamber as shown in Fig 3.1a. The results of these measurements are shown in Fig 3.1b. As may be seen, the model tests showed a relatively small shock front attenuation in the straight tunnel section (MP 7 - 9) whereas the full scale results showed a considerable reduction. This unexpected result caused initially a suspicion that the reading from the pressure gauge nearest to the exit had been erroneous.

However, subsequent calculations of the front pressures from arrival time data confirmed to

within approximately  $\pm 20\%$  the earlier average peak pressure readings /15/ as seen from Fig 3.1b. The large attenuation observed in the outer parts of the tunnel has been analysed elsewhere /3/ and found to be qualitatively due to the large wall roughness. This will be discussed shortly, but first we will show the results from two other large scale tests in tunnel systems with similar wall roughness. The geometries and the positions of the measuring points in these tests are shown in Fig 3.1c and 3.1d.

The tunnels were blasted out of rock with hydraulic diameters approximately  $D = 2,7 \text{ m}$  /16/ and  $D = 6 \text{ m}$  /10/. The average height of wall roughness elements was approximately  $\bar{e} = 0,2 \pm 0,1 \text{ m}$  (defined in Sec 2.5) and comparable to the wall roughness in the "Operation Block" test.

In the 2,7 m diameter tunnel system, TNT charges ranging from 100 kg to 1000 kg were detonated near the dead end of the tunnel, whereas in the 6 m diameter tunnel TNT charges ranging from 1 kg to 92 kg were detonated near one of the exits. Fig 3.1e shows typical peak pressure data versus distance in tunnel diameters for these tests (defined in Figs 3.1a, 3.1c, and 3.1d) together with the "Operation Block" data.

For details regarding data reduction, reference is made to the original reports. It should, however, be pointed out that the average peak pressure data in Fig 3.1e were found directly from the pressure-time recordings by taking the mean values of the pressures of peaks and troughs of the pressure oscillating system. The data found from shock front velocity measurements will also correspond qualitatively to this definition.



As may be seen from Fig 3.1e, the blast attenuation is significant for all three tests and as will be discussed shortly, a large part of this is due to a relatively large wall roughness. Unfortunately, the results extend out to moderate distances in tunnel diameters and this complicates a direct comparison with the model discussed in Sec 2. To get further insight into the long range effects of wall roughness attenuation we shall first turn to some earlier test results in straight tubes, and return in Sec 3.3 to the data in Fig 3.1e.

### 3.2 Tests in a 0,05 m Diameter Tube

The long range effects of wall roughness attenuation have been reported earlier for detonations inside a  $D = 0,05$  m steel tube where measurements were extended out to approximately  $L/D = 700 / 10/$ . To analyse these earlier results, the peak pressure data were fitted to the theoretical expression in Fig (2.5d) and the empirical results in Eq (2.6b) as follows:

The smooth-wall pressure was assumed to vary as

$$p_0 = C_1(Q/V_t)^{C_2} \quad (3.2a)$$

and the wall roughness attenuation was assumed to be governed by the impedance function

$$Y(p_0) - Y(p) = 2\epsilon \frac{\bar{e}}{D} \frac{L}{D} \quad (3.2b)$$

Here,  $p_0$  is the fictitious smooth wall pressure at a distance  $L$  from the charge and  $p$  the actual measured pressure.  $C_1$ ,  $C_2$ , and  $2\epsilon \bar{e}/D$  were treated as fitting parameters. To simplify the calculations it was assumed that  $\epsilon = 1/2$  (See Sec 2.5). The results of the fitting procedure are shown in Figs 3.2a and 3.2b. As may be seen, measurements of the attenuation appear to be consistent with the

proposed model. In particular, the average wall roughness was found to be  $\bar{e} = 0,46 \pm 0,05$  mm which compares favourably with the direct estimated value of  $\bar{e} = 0,3$  mm /10/. The data points in Fig 3.2a appear to lay on a smooth falling curve with no kinks as postulated for a constant pressure wave (Sec 2.5). In particular, the feedback distance using Eq (2.5n) is found to be  $(L/D)_F = 75$ . The results in Fig 3.2a show that there is no distinct kink at approximately this distance. If a constant pressure wave had been assumed, i.e.  $p_0 = \text{constant}$  in Eq (3.2a), the use of Eq (2.5d) would have approximately been consistent with a transition from  $\epsilon = 1$  to  $1/2$  at  $L/D = 178$  and an  $\bar{e} = 0,6$  mm. The results of this analysis are shown in Fig 3.2c. This shows the one has to be careful in attempting to analyse peaked pressure waves only in terms of Eq (2.5d).

### 3.3 Analysis of Test Results in Tunnels

Now we shall return to the large scale results in tunnels in Fig 3.1e. The data for the  $D = 2,7$  m and  $D = 6$  m tunnels were analysed using Eq (3.2a) and (3.2b) as for the  $D = 0,05$  m tube and the results are shown in Fig 3.2d in terms of the impedance function and in Fig 3.2e using the pressures explicitly.

The average wall roughness was found to be  $\bar{e} = 0,12$  m for the  $D = 2,7$  m tunnel and  $\bar{e} = 0,15$  m for the  $D = 6$  m tunnel.

This would correspond to an average height of the maximum roughness elements  $e_{\max} = 2\bar{e} \approx 0,3$  m in Fig 2.5c. This appears to be quite consistent with direct observation of the tunnel walls.

As for the "Operation Block" results in Fig 3.2d the data are really too few in the straight tunnel to do the same kind of fitting procedure. We have therefore tentatively shown the attenuation one would expect for an average roughness of  $\bar{e} = 0,17$  m or  $2\epsilon\bar{e}/D = 0,1$ .

The "smooth wall" curve a) was estimated from case d) in Fig 2.6b. As may be seen, the attenuation appears to be somewhat larger than the prediction of curve b). This may possibly be due to large amounts of dust and water in the tunnel system /3/ or special effects due to the particular geometry in this test /17/.

The phenomenological description of blast in tunnels also included a diffraction region, a build-up region, and a turbulent choke. This model applied strictly only to a tunnel adjacent to an infinite half space. Clearly, for detonation inside a tunnel or in a chamber adjacent to the tunnel as for the tests reported here, the situation is somewhat different. In particular, the turbulent choke formation with a build-up pressure  $p_B$  and a "choked" overpressure  $p_C$ , would according to Eq (2.4) require a large pressure drop out to 20 tunnel diameters or so. /7/. The present data do not appear to support this effect. The observed reduction in pressure seems to be due only to diffraction, impedance (roughness), and rarefaction, but it is hardly possible to be more specific at this point.

The possible implications of wall roughness attenuation on external safety distances has been discussed briefly in Ref 3 in connection with the "Operation Block" test, but it is of interest to give a more general discussion. This will be the subject of Sec 4.



#### 4. EFFECTS OF TUNNEL ROUGHNESS ON EXTERNAL SAFETY DISTANCES

Measurements of the blast propagation outside models of underground storage sites /18/ and shock tubes /19, 20/ have shown that the isobar distances from the exit are primarily dependent on the exit pressure. In particular it has been proposed that the external safety distances or 50 mbar isobar distances can be approximated by /21/:

$D_5/D = 18 p_e^{0,67}$	Sector	$0^\circ - 30^\circ$	
$D_4/D = 15 p_e^{0,67}$	Sector	$30^\circ - 50^\circ$	
$D_3/D = 12 p_e^{0,67}$	Sector	$60^\circ - 90^\circ$	
$D_2/D = 8 p_e^{0,67}$	Sector	$90^\circ - 120^\circ$	
$D_1/D = 4,5 p_e^{0,67}$	Sector	$120^\circ - 180^\circ$	(4.a)

Here,  $D$  is the effective main passageway diameter in meters and  $p_e$  the exit pressure in bars. The angles are measured from the extended centerline of the main passageway as shown in Fig 4.a, and  $D_1$ - $D_5$  are the safety distances in meters from the exit.

It is of interest to see the effects of wall roughness attenuation on the safety distances using the model outlined in Sec 3.2. Consider the connected chamber storage site in Fig 4.b which is scaled up from an earlier model in a linear scale 1:100 /18/. The model tests showed the pressure in the main passageway could be fitted empirically to /12/:

$$p_o = 4,3 (Q/V_t)^{0,55} \quad (4.b)$$

with  $Q$  and  $V_t$  defined in Fig 4.b. This result then is valid for an essentially smooth-walled tunnel.



In the event of significant wall roughness,  $\bar{e}/D$ , we shall use the model proposed in Sec 3.2:

$$Y(p) = Y(p_0) - 2\epsilon \frac{e}{D} \frac{L}{D} \quad (4.c)$$

Here,  $p_0$  is fictitious pressure at a distance  $L/D$  defined in Eq (4.b) and  $p$  the pressure at the same distance including the wall roughness. The efficiency factor  $\epsilon$  is defined as

$$\epsilon = 1 \quad \text{for } L/D \leq (L/D)_F$$

$$\epsilon = 1/2 \quad \text{for } L/D > (L/D)_F,$$

where  $(L/D)_F$  is the feedback distance determined from Eq (2.5n). The results of these calculations are shown in Fig 4.c for values of  $\bar{e}/D$  ranging from 0,01 to 0,1.

As an example, we choose  $L/D = 20$  and use the corresponding pressures  $p$  as the exit pressures  $p_e$  in Eq (4.a) to estimate the corresponding safety distances which are given in Table 4.a. This is displayed graphically in Fig 4.d. As may be seen, even a moderate wall roughness reduces the distances significantly.

It should be cautioned that these results are based on the assumption of a steady state blast propagation in the tunnel. As pointed out in Sec 2, there will obviously be a very complicated diffraction region in the first few tunnel diameters near the exit of the branch passageway. However, from the analysis in Sec 3 the present model appears to qualitatively reproduce the earlier results which partly justifies the extension to the more general situation discussed here.

## 5. CONCLUSIONS

The main purpose of the present report has been to provide experimental results which confirm that a macroscopic surface roughness in tunnels attenuate front pressures of blast waves significantly. Thus wall roughness provides a degree of control for reducing the hazardous area around an underground ammunition storage site.

Using a semi-empirical theory for steady turbulent flow in rough pipes in combination with empirical results from model tests, it has been possible to reproduce the results in tunnels blasted out of rock.

Various empirical cross checks of the the results in tunnels with diameters ranging from 2,7 m to 6 m have produced an average wall roughness of  $\bar{e} = 0,15 \pm 0,05$  m.

For a typical underground ammunition storage this roughness could easily reduce the hazardous area by a factor of two or more compared to an essentially smooth-walled site. These aspects should therefore be carefully considered by the design engineer to reduce the safety distances to a minimum at minimum cost.

## REFERENCES

1. E. Abrahamsson, "Operation Block",  
Royal Swedish Fortification Administration,  
Research Dept, Stockholm 80,  
Report No 119:5 (1974).
2. E. Abrahamsson, "Operation Block",  
Proceedings Fourth International Symposium on Military  
Applications of Blast Simulation, paper D 1.  
Atomic Weapons Research Establishment  
Foulness, England (1974).
3. A. Rinnan, A.T. Skjeltnorp and A. Jenssen,  
"Underground Ammunition Storage. Model Test to Investi-  
gate the Strength and Effectiveness of a Selfclosing  
Concrete Block",  
Report no 98/74, Norwegian Defence Construction Service,  
Oslo (1974).
4. A. Rinnan, A.T. Skjeltnorp and A. Jenssen,  
"Underground Ammunition Storage. Model Test to Investi-  
gate the Strength and Effectiveness of a Selfclosing  
Concrete Block",  
Proceedings Fourth International Symposium on Military  
Applications of Blast Simulation, paper D 2.  
Atomic Weapons Research Establishment,  
Foulness, England (1974).
5. A.R. Kribel,  
"Airblast in Tunnels and Chambers",  
Defence Nuclear Agency  
Washington D.C. Report DASA 1200 - II  
Supplement 1 (AD 906986) (1972).
6. A.T. Skjeltnorp, T. Hegdahl and A. Jenssen,  
"Underground Ammunition Storage. Report I",  
Report no. 80/72, Norwegian Defence Construction Service  
(1975).
7. F.B. Porzel,  
"Study of Shock Impedance Effects in a Rough Walled  
Tunnel",  
Institute for Defence Analysis, Research Paper P-330.  
(1969). (AD 684790).
8. R.J. Emerich and C.W. Curtis,  
"Attenuation in Shock Tube",  
J. Appl. Phys. 24, 360 (1953).
9. A. Skjeltnorp,  
"One-Dimensional Blast Wave Propagation",  
Norwegian Defence Construction Service, Report No 48/69.  
(1969).



10. A.T. Skjeltorp and A. Jenssen,  
"One-Dimensional Blast Wave Propagation",  
Proceedings Fourth International Symposium on Military Applications of Blast Simulation, Paper D 5,  
Atomic Weapons Research Establishment,  
Foulness, England (1974).
11. A.T. Skjeltorp, T. Hegdahl and A. Jenssen,  
"Underground Ammunition Storage. Report III",  
Report no. 81/72, Norwegian Defence Construction Service  
(1975).
12. A.T. Skjeltorp, T. Hegdahl and A. Jenssen,  
"Underground Ammunition Storage. Report IV",  
Report no. 82/72, Norwegian Defence Construction Service  
(1975).
13. A.T. Skjeltorp, T. Hegdahl and A. Jenssen,  
"Underground Ammunition Storage. Report II",  
Report no. 79/72, Norwegian Defence Construction Service  
(1975)
14. D.L. Lehto and L. Rudlin,  
"Differences between Nuclear and HE Weapons Effects",  
Proceedings Fourth International Symposium on Military Applications of Blast Simulation, Paper D 5.  
Atomic Weapons Research Establishment,  
Foulness, England (1974).
15. C. Svensson. Private Communication.
16. K.G. Schmidt,  
"Underground Explosion Trials at Raufoss 1968: Blast Wave Propagation Following a Detonation in a Tunnel System",  
Norwegian Defence Research Establishment, Report X-128.  
(1970).
17. G. Gürke,  
"Analyse der Druckmessungen aus Modell- und Prototypenversuchen zur Lagerstollenerprobung in Trängslet",  
Bericht Nr. E 1/74, Ernst-Mach-Institut, Freiburg.
18. G. Fredrikson and A. Jenssen,  
"Underground Ammunition Storage",  
Report no. 59/70, Norwegian Defence Construction Service  
(1970).
19. D.J. James,  
"An Investigation of the Pressure Wave Propagated from the Open End of a 30 x 18 in Shock Tube",  
Atomic Weapons Research Establishment (AWRE), Report no. O-60/65, United Kingdom Atomic Energy Authority,  
(1965).

20. B.P. Bertrand, W.T. Matthews,  
"Free Field Overpressures Resulting from Shock Waves  
Emerging from Open-Ended Shock Tubes",  
Ballistic Research Laboratories, Memorandum Report,  
October 1965.
21. Informal Working Paper, NATO Underground Storage,  
Sub-Group AC/258.  
Norwegian Defence Construction Service,  
October 1974.

$\bar{e}/D$	$p_e$ (bar)	$D_5$ (m)	$D_4$ (m)	$D_3$ (m)	$D_2$ (m)	$D_1$ (m)	Hazardous area 1000 m <sup>2</sup>	Relative
0	35	975	866	650	433	244	1271	1
0,02	18	624	555	416	277	156	522	0,41
0,04	10	421	374	281	187	105	237	0,19
0,06	6	299	266	199	133	75	120	0,09
0,08	3,7	216	192	144	96	54	63	0,05
0,10	2,5	166	148	111	74	42	37	0,03
		$D_5/D = 18p_e^{0,67}$	$D_4/D = 16p_e^{0,67}$	$D_3/D = 12p_e^{0,67}$	$D_2/D = 8p_e^{0,67}$	$D_1/D = 4,5p_e^{0,67}$		

Table 4.a Safety distances outside an underground ammunition storage site for various tunnel wall roughness as discussed in the text.



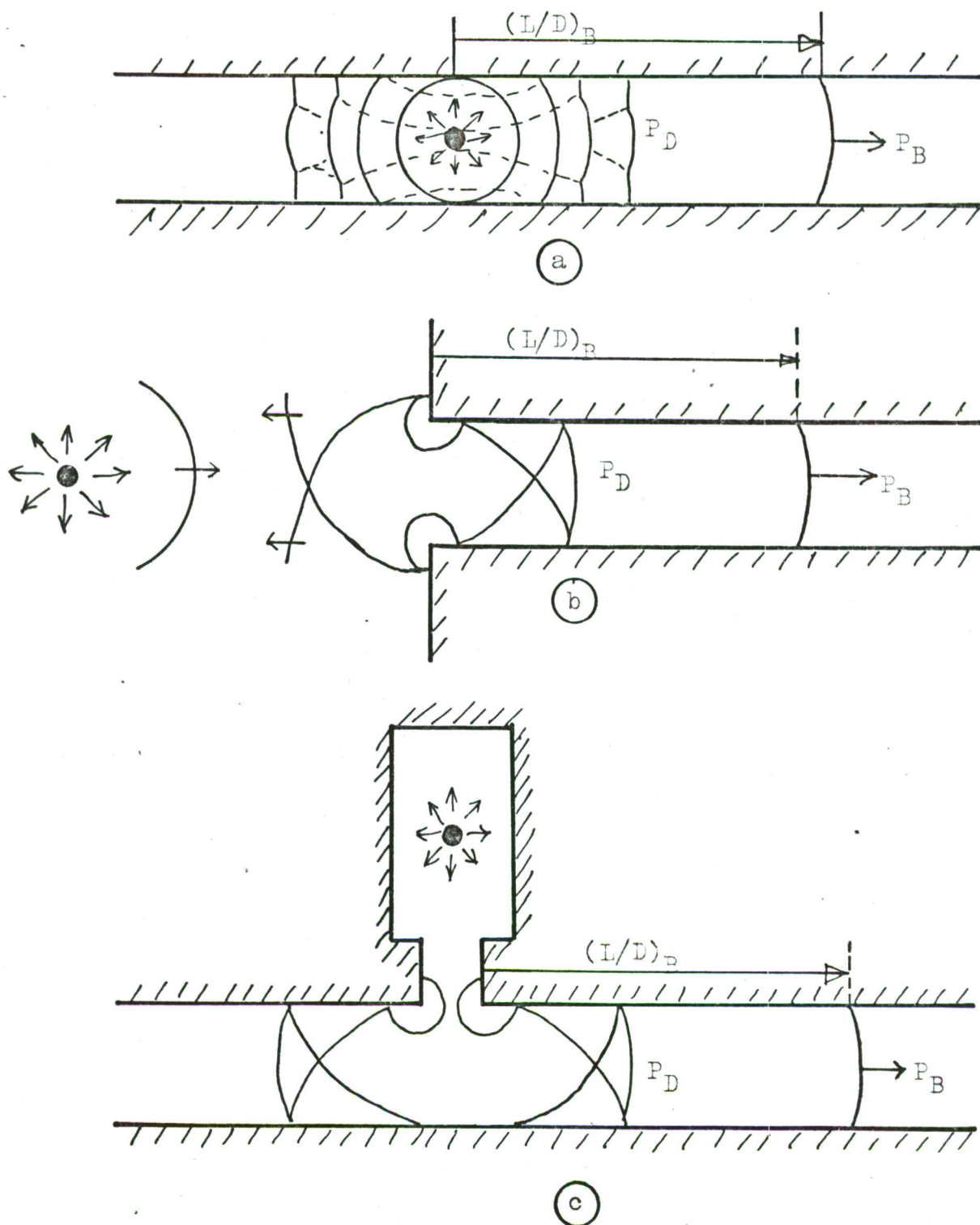


Fig.2.1 Shock front diffraction patterns shown schematically for:

- a) Detonation of a charge in a straight tunnel.
- b) Shock wave entering a tunnel.
- c) Detonation of a charge in an underground ammunition storage chamber.

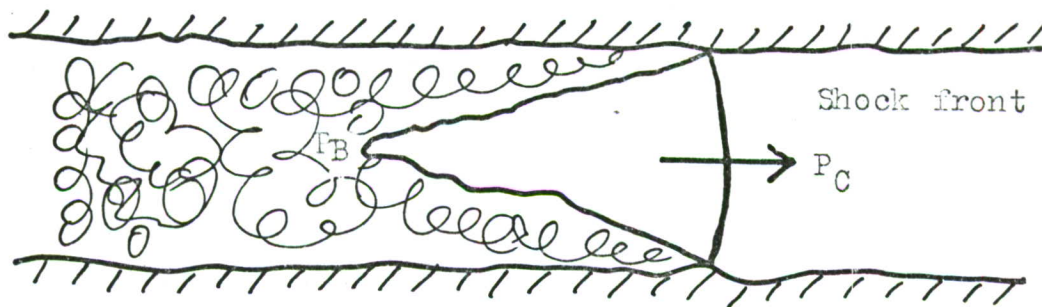


Fig.2.4 Turbulent choke formation in a tunnel.

$P_C$  is the "choked" overpressure at the shockfront,  
and  $P_B$  is the buildup pressure.

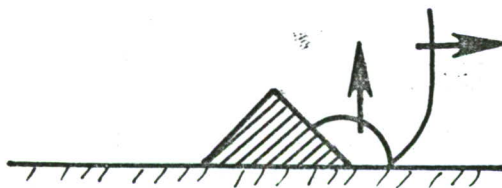
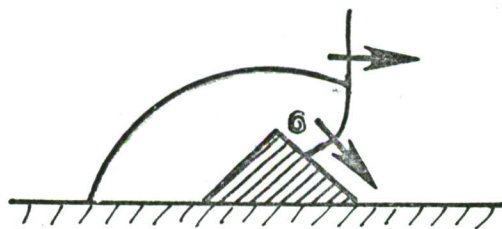
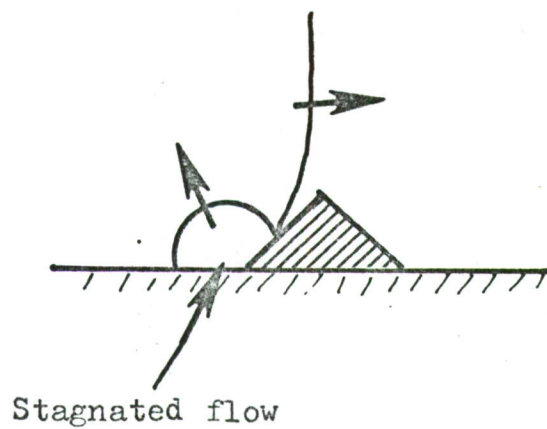


Fig.2.5a Shock wave passing an idealized roughness element.



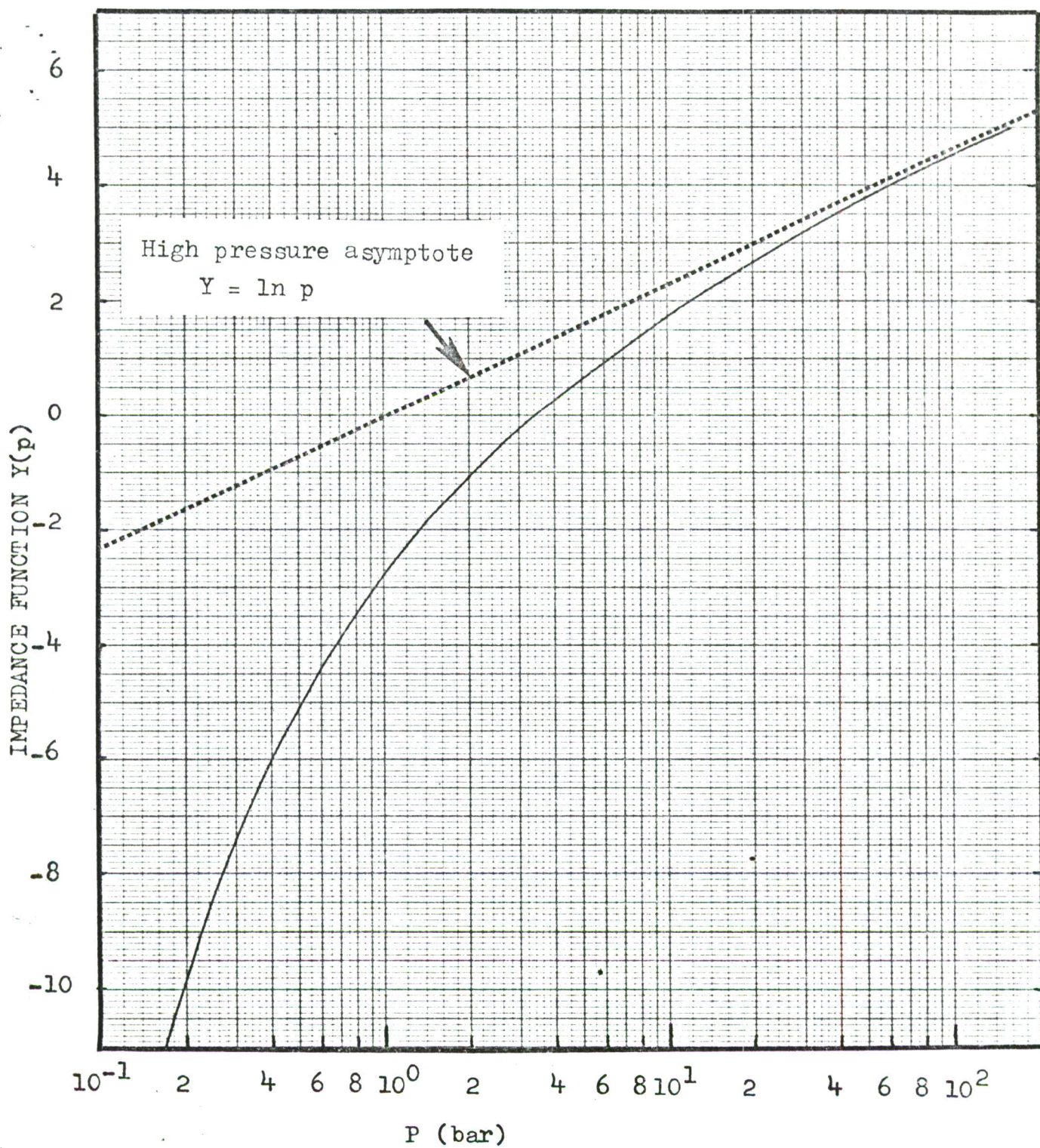


Fig.2.5b. Impedance function  $Y(p)$  as defined in Eq. (2.5g) versus overpressure  $p$ .

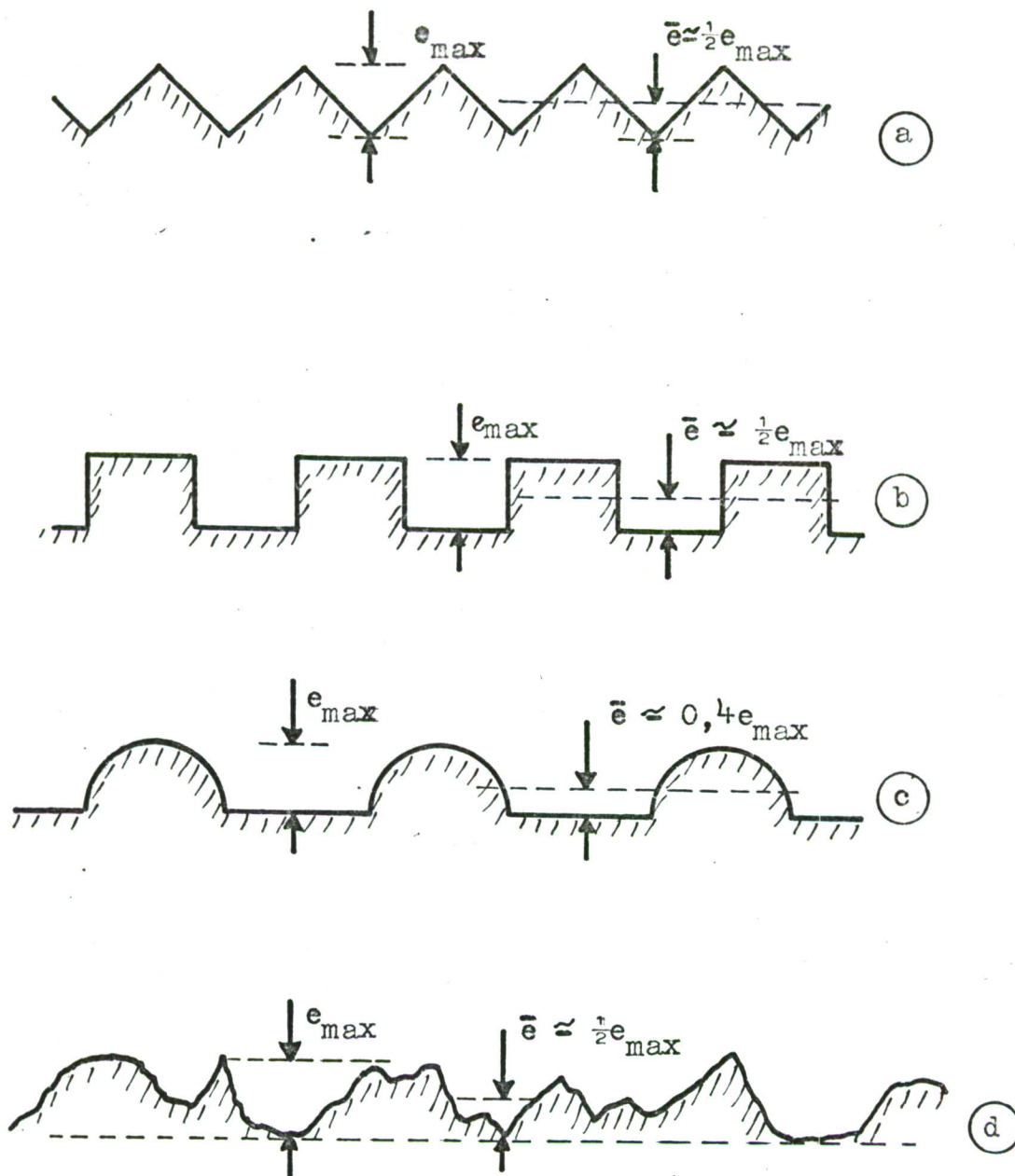


Fig. 2.5c Idealized examples of wall roughness in a), b), c).  
 $e_{\max}$  is the maximum height of roughness elements  
and  $\bar{e}$  the average wall roughness estimated from  
Eq.(2.5m) assuming  $\bar{e} \ll D$ . For a realistic wall roughness  
in d), a reasonable estimate of  $\bar{e}$  is  $\frac{1}{2} \bar{e}_{\max}$ .



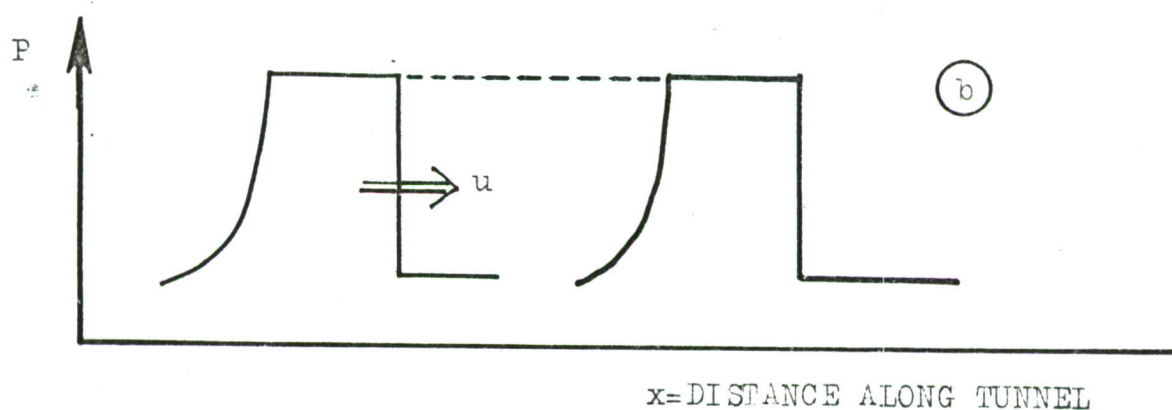
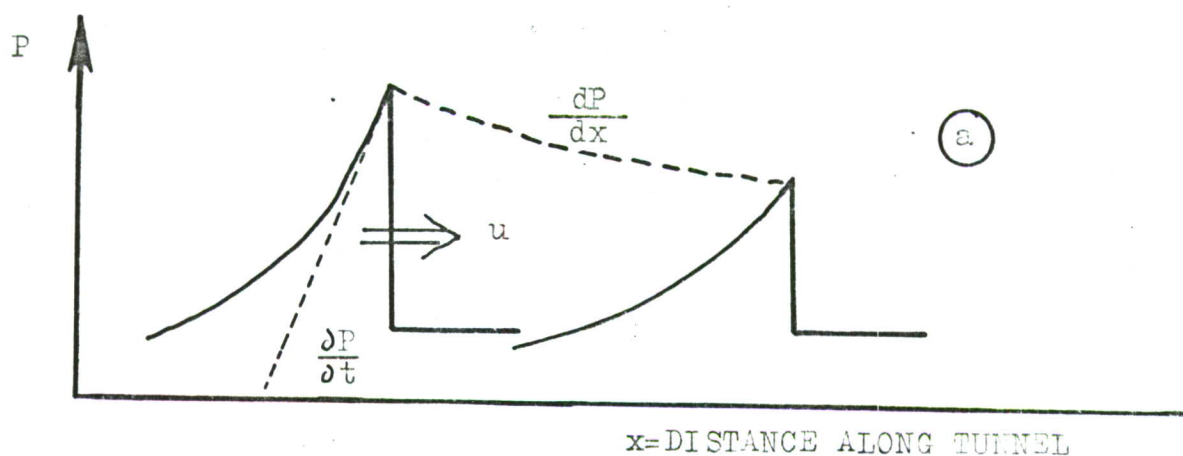

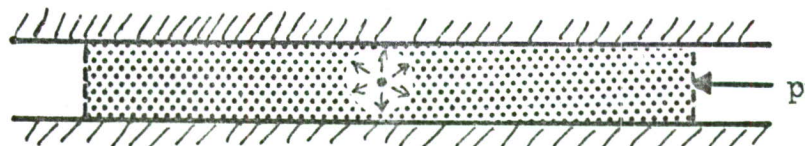


Fig.2.6a In a) the shock front is attenuated due to the rarefaction waves whereas in b) (typical for an air-driven shock tube) no attenuation will take place.



  $V_t$  = total volum

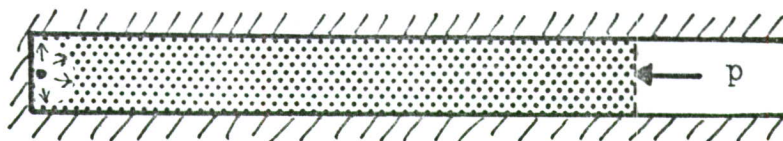
(a)



Tests in tubes/tunnel /10/:

$$p \approx (15,4 \pm 1,0) (Q/V_t)^{0,66 \pm 0,02}$$

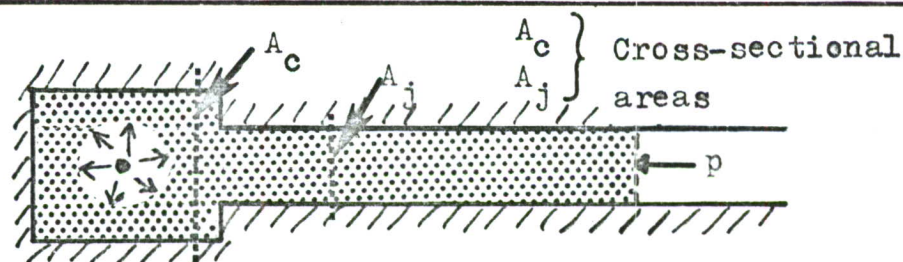
(b)



Deduced from (a) /10/:

$$p \approx 24 (Q/V_t)^{0,66}$$

(c)

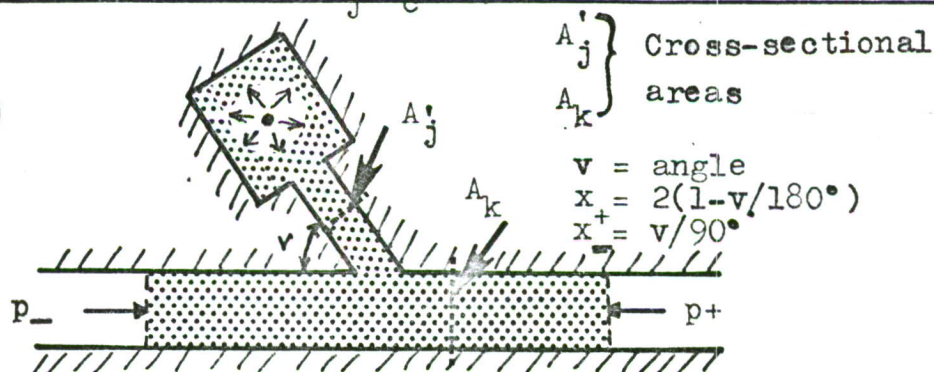


Model tests /11/:

$$p = (12,1 \pm 0,6) (Q/V_t)^{0,61 \pm 0,02} (A_j/A_c)^{0,19 \pm 0,04}$$

$$\text{Range : } 0,11 \leq A_j/A_c \leq 0,45$$

(d)



$$v = \text{angle}$$

$$x = 2(1-v/180^\circ)$$

$$x^+ = v/90^\circ$$

Model tests /12/:

$$p = (10,0 \pm 0,6) (QX_+/V_t)^{0,55 \pm 0,02} (A'_j/A'_k)^{0,61 \pm 0,06}$$

$$\text{Range: } 35^\circ \leq v \leq 90^\circ ; 0,125 \leq A'_j/A'_k \leq 0,5$$

Fig.2.6b The results from various model tests show that the front pressure in the tunnel systems of underground storage sites with certain limitations can be expressed empirically as  $p = f(a_1, a_2, \dots) (Q/V_t)^{C_2}$ , where  $C_2 = 0,6 \pm 0,1$  and a proportionality factor  $f(a_1, a_2, \dots)$  containing geometrical parameters.



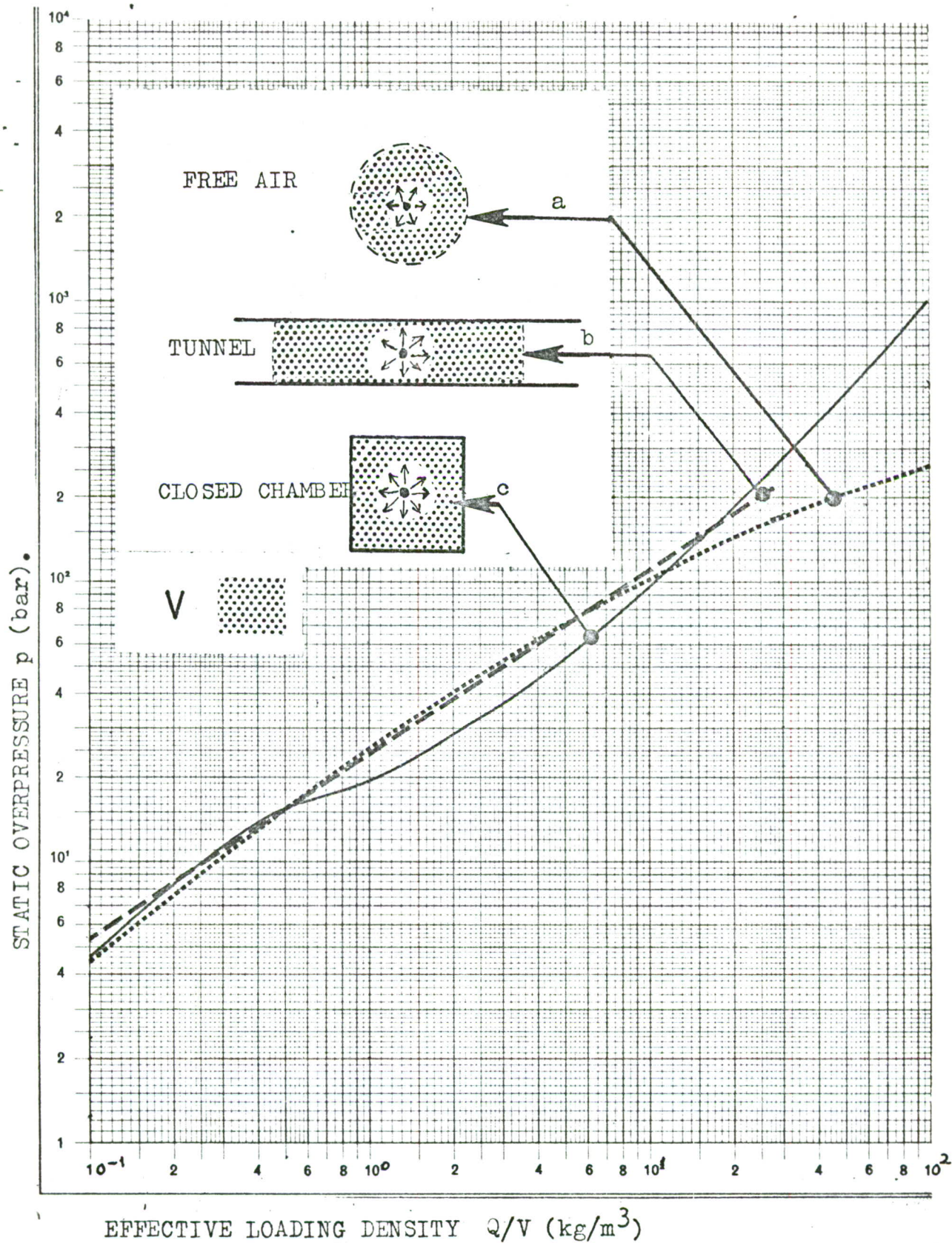
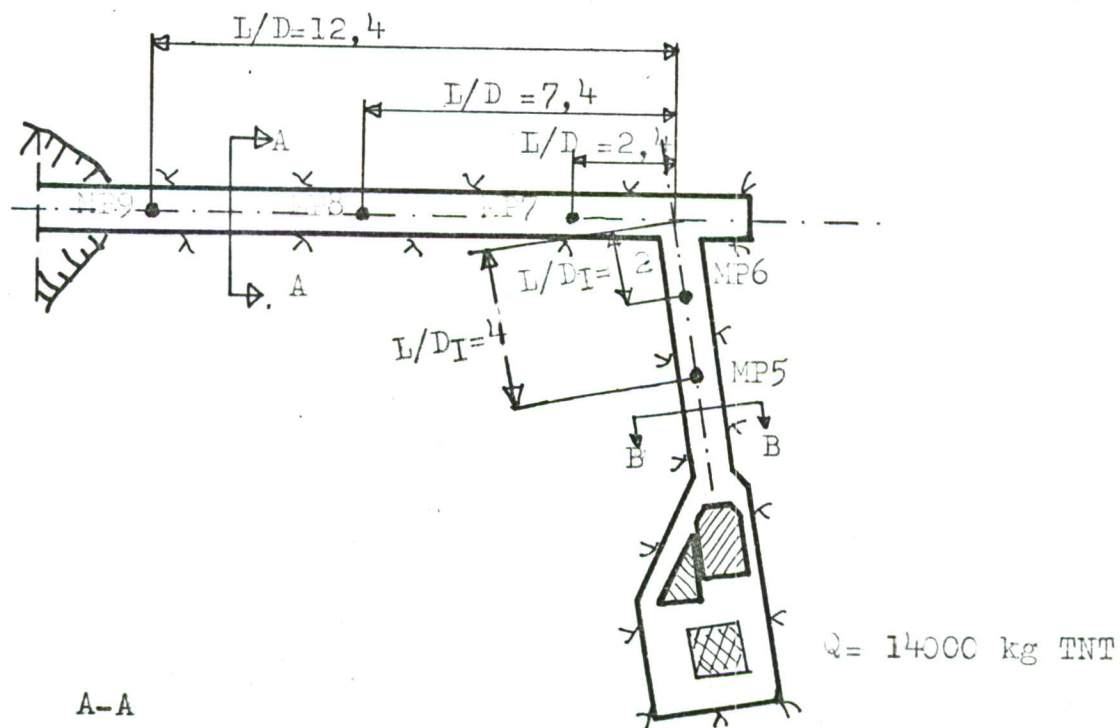


Fig.2.6c Static overpressure versus effective loading density for TNT detonation in:

- a) Free air /14/.
- b) Tubes/tunnels /10/.
- c) Closed chamber /13/.



A-A



CROSS-SECTIONAL AREA  $A = 11,3 \text{ m}^2$   
 HYDRAULIC DIAMETER  $D = 3,4 \text{ m}$

B-B



CROSS-SECTIONAL AREA  $A_I = 8,6 \text{ m}^2$   
 HYDRAULIC DIAMETER  $D_I = 3,0 \text{ m}$

Fig.3.1a Tunnel system and measuring points in the "Operation Block" test/1,2/.



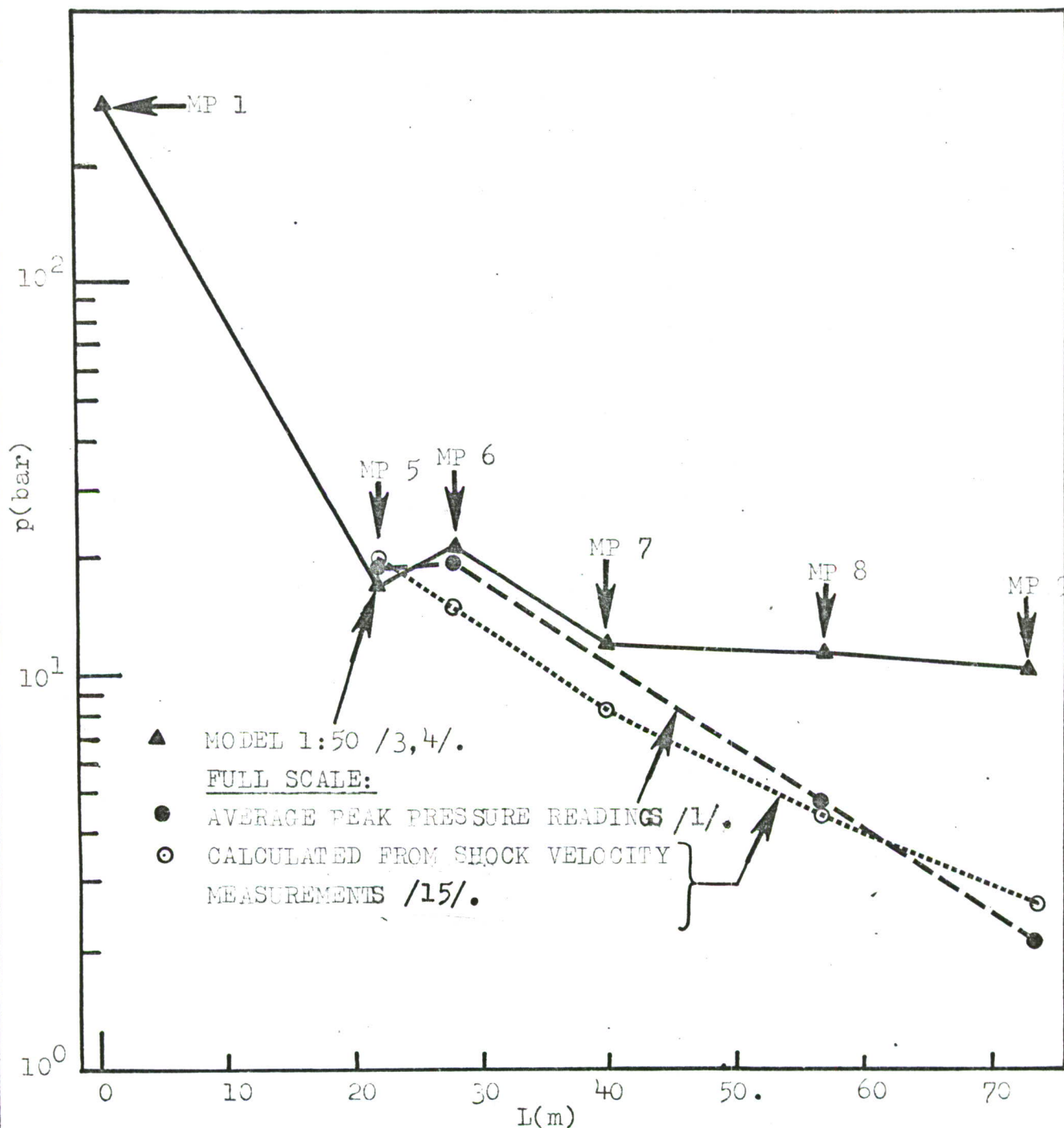
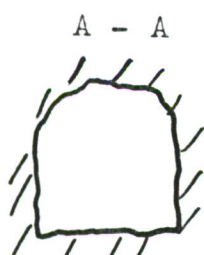
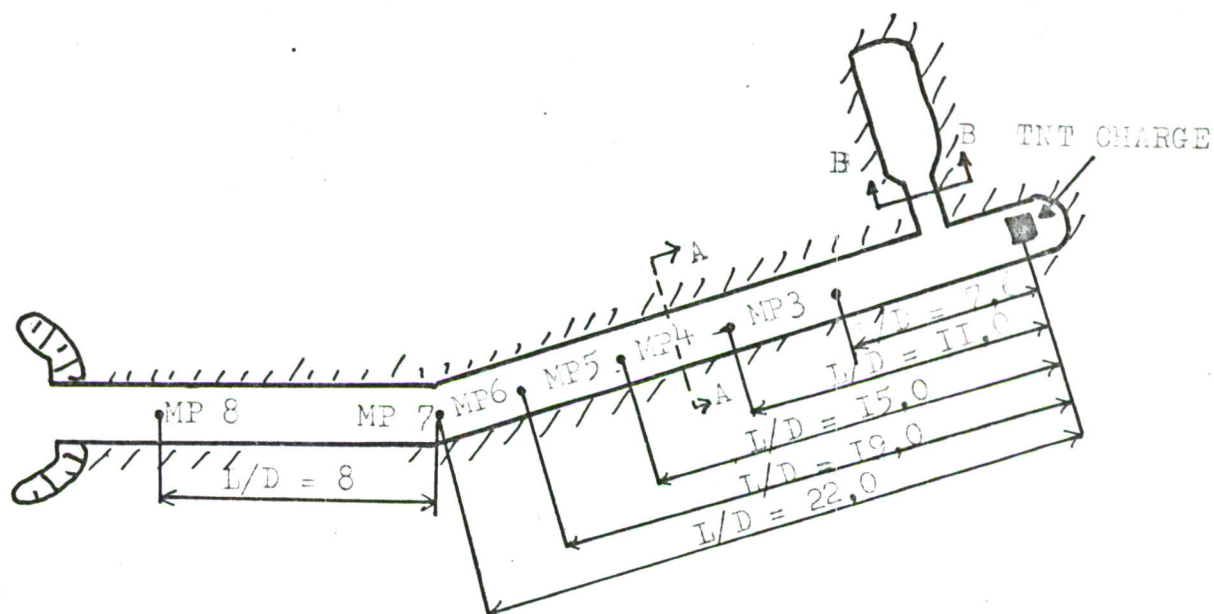


Fig.3.1b Average peak pressure in a tunnel system versus distance from the entrance to the detonation chamber in the "Operation Block" tests, see Fig.3.1a. The full scale data show a much larger blast wave attenuation near the tunnel exit than the model data.

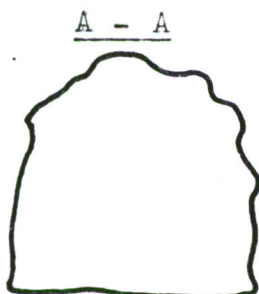
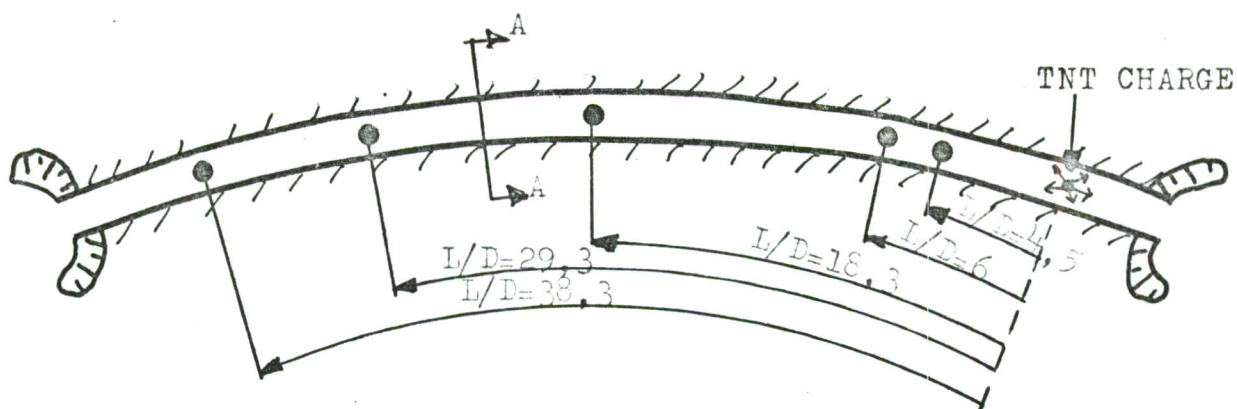


CROSS-SECTIONAL AREA  $A = 5,5\text{m}^2$   
 HYDRAULIC DIAMETER  $D = 2,7\text{m}$



CROSS-SECTIONAL AREA  $A_I = 2,4\text{m}^2$

Fig.3.1c Tunnel system and measuring points in the Raufoss trials /16/.



CROSS-SECTIONAL AREA  $A \approx 28\text{m}^2$   
HYDRAULIC DIAMETER  $D \approx 6\text{m}$

Fig.3.1d Blast propagation test in an abandoned railway tunnel ( radius of curvature approximately 200m )  
/9,10/.



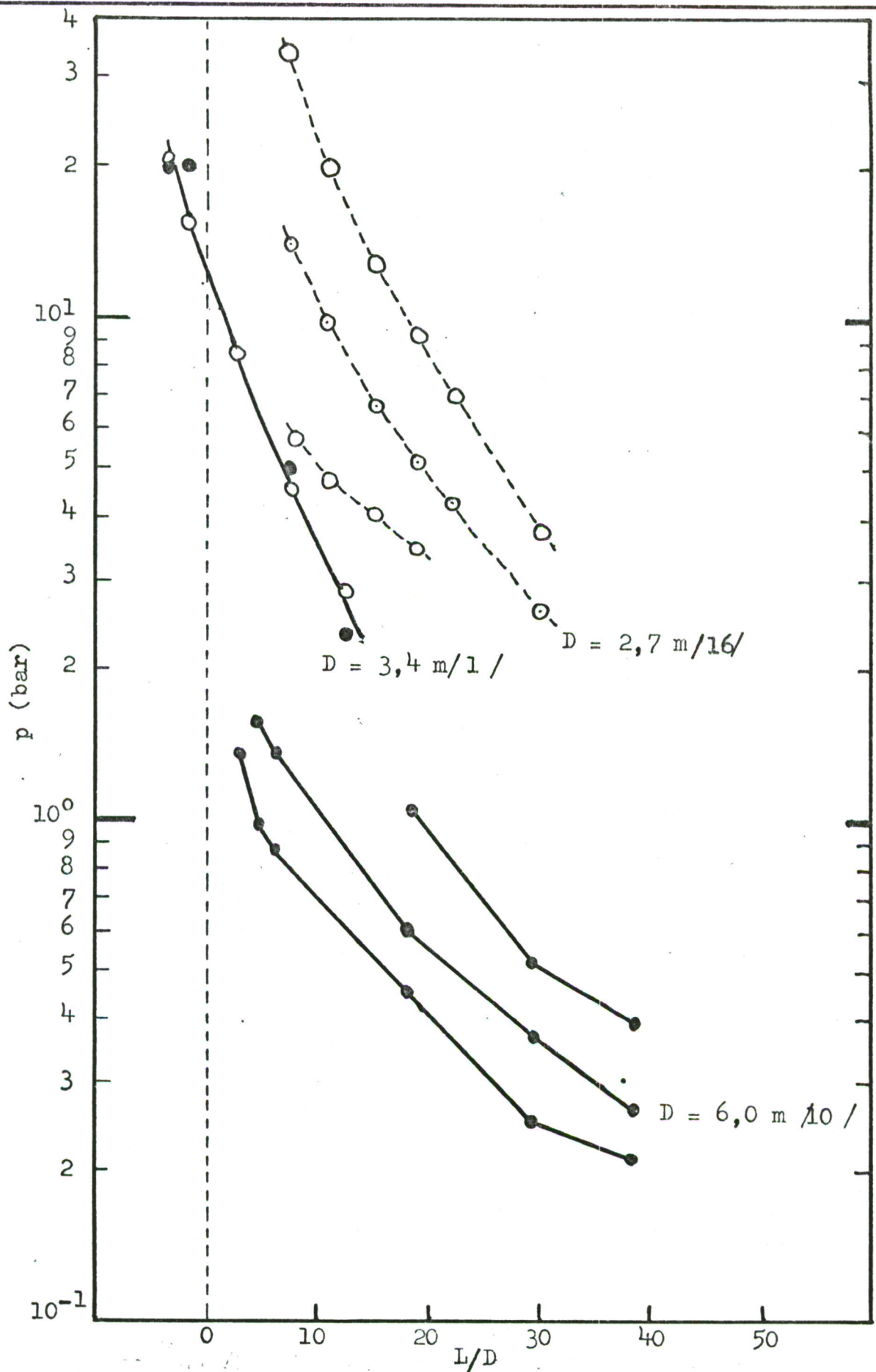


Fig.3.1e Average peak overpressure versus tunnel distance in diameters for three tests with:

$D = 2,7 \text{ m}$  ( $Q = 100, 300, \text{ and } 1000 \text{ kg TNT}$ )

$D = 3,4 \text{ m}$  ( $Q = 14000 \text{ kg TNT}$ )

$D = 6,0 \text{ m}$  ( $Q = 15, 30, \text{ and } 92 \text{ kg TNT}$ )

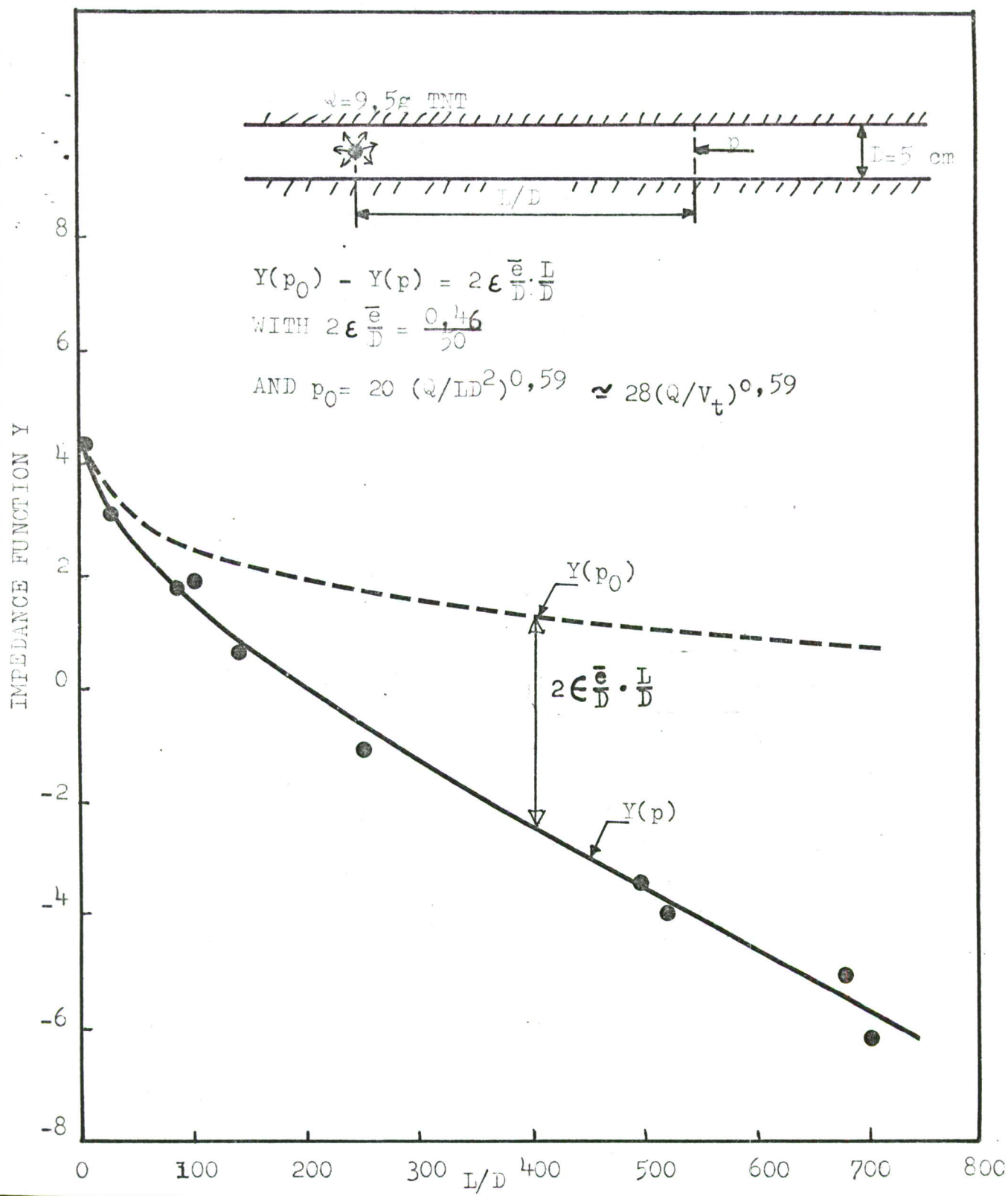


Fig.3.2a Peak pressure attenuation of the blast from 9,5g TNT! detonated in a 5 cm diameter tube expressed as the impedance function  $Y$  versus tube length in diameters.

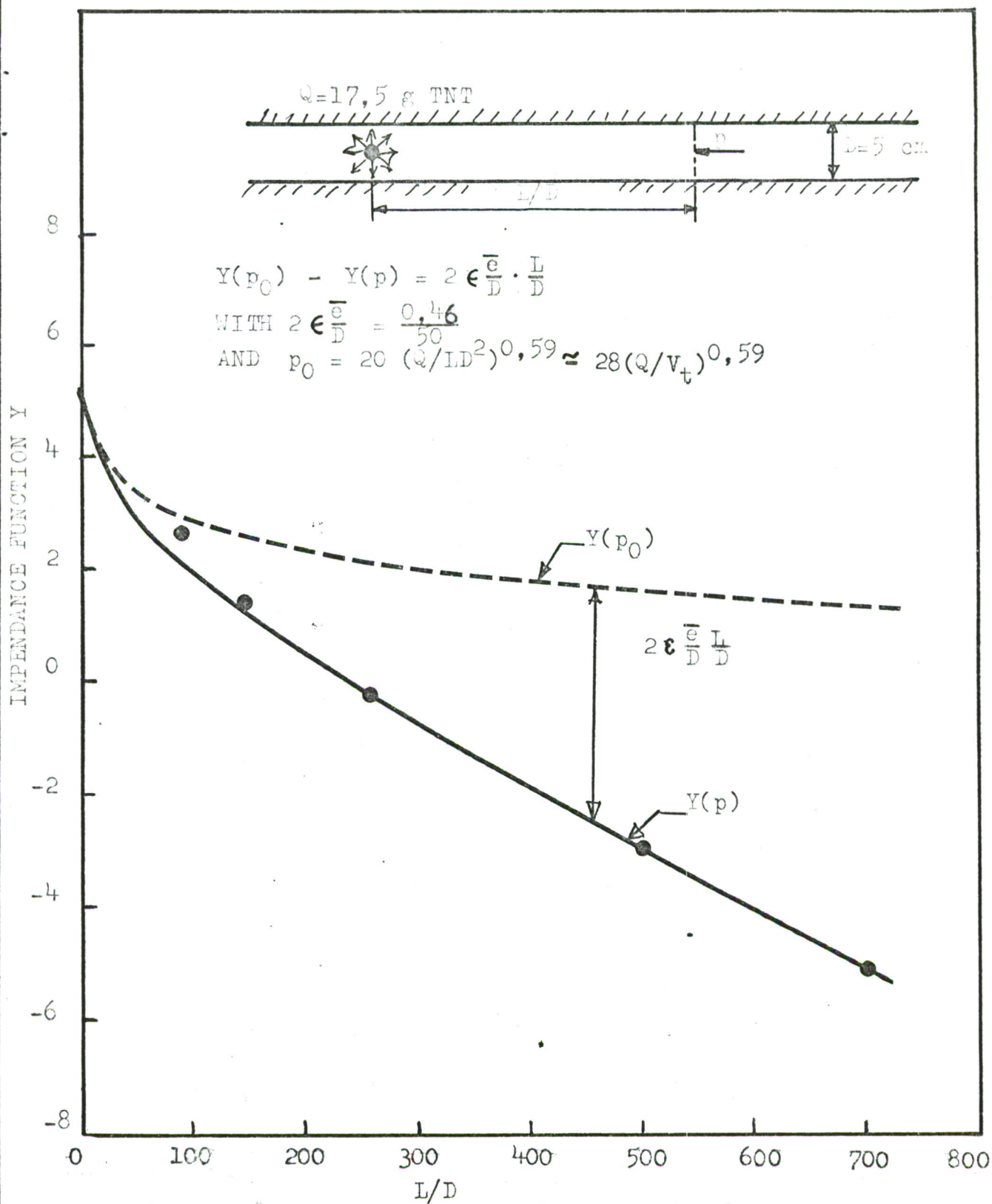


Fig.3.2b Peak pressure attenuation of the blast from 17,5g TNT detonated in a 5 cm diameter tube expressed as the impedance function Y versus tube length in diameters.



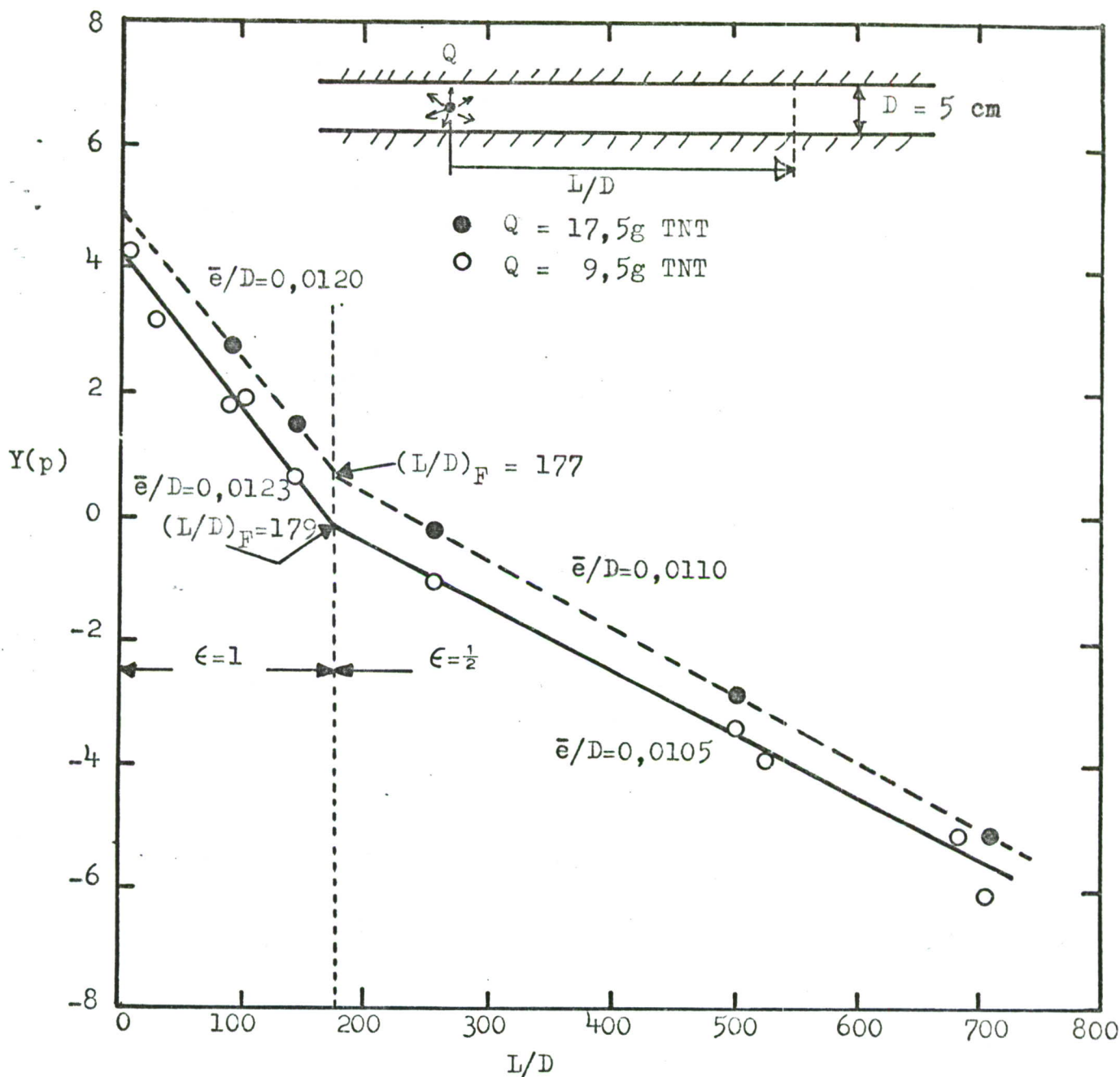


Fig.3.2c Test of proposed impedance theory for TNT detonation inside a  $D = 5\text{ cm}$  diameter steel tube disregarding attenuation due to the rarefaction wave. The straight lines represent least square fits to the data for distances below and above a feedback distance  $(L/D)_F \approx 178$  with an efficiency factor  $\epsilon = 1$  and  $\epsilon = \frac{1}{2}$ , respectively. The four fitted values of  $\bar{e}/D$  produce  $\bar{e}/D = 0,0115 \pm 0,0008$  for all the data, or an average wall roughness  $\bar{e} = 0,58 \pm 0,04\text{ mm}$  which is about 25 % higher than the value for  $\bar{e}$  found in Figs. 4.2a and 4.2b where also the effects from the rarefaction wave were considered.

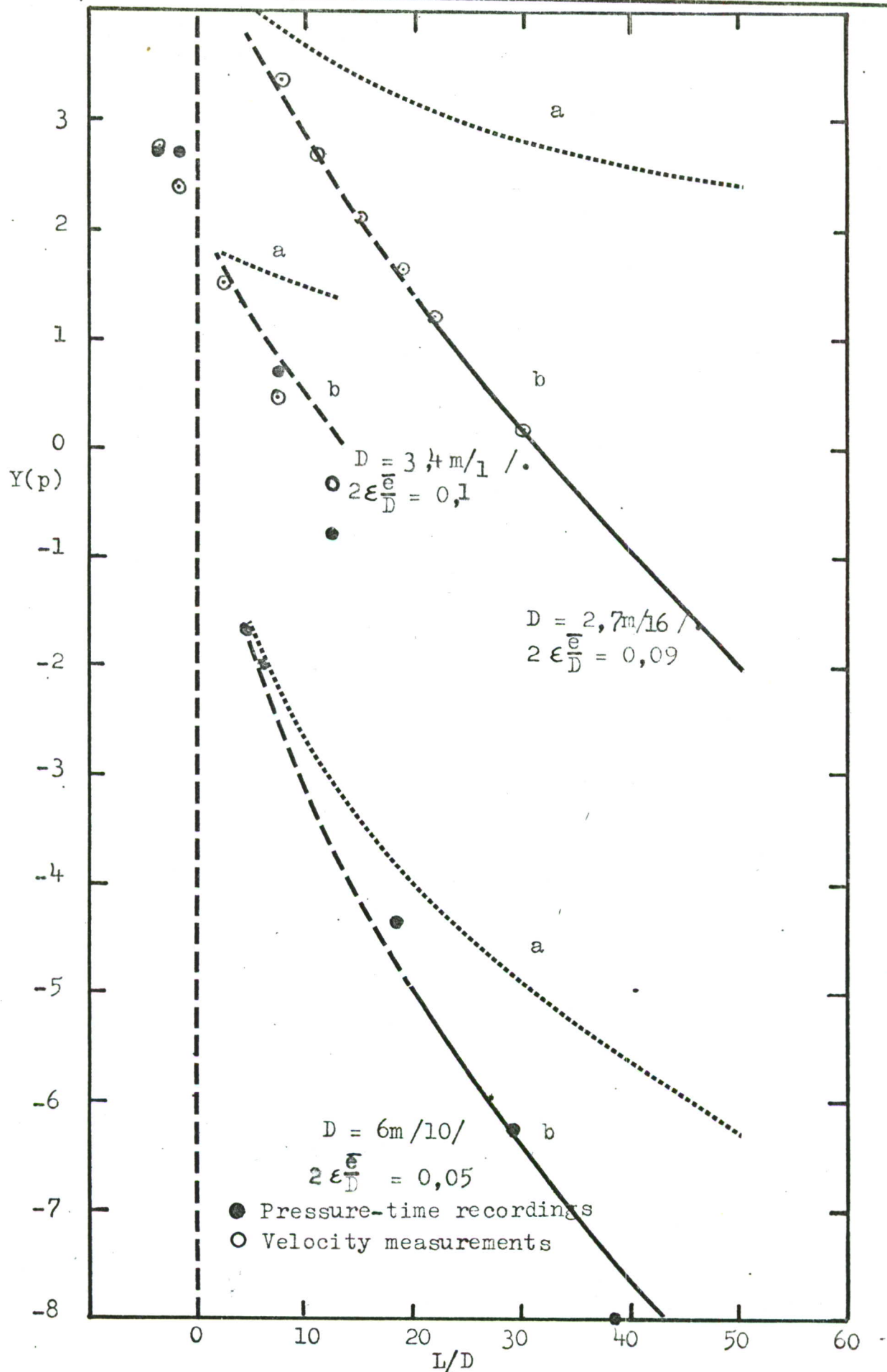


Fig.3.2d. Impedance function  $Y(p)$  versus tunnel length in diameters for three large scale tests. Curves a) indicate the attenuation for smooth-walled tunnels, Eq.(3.2a), whereas curves b) show the total attenuation including also wall roughness using Eq.(3.2b).

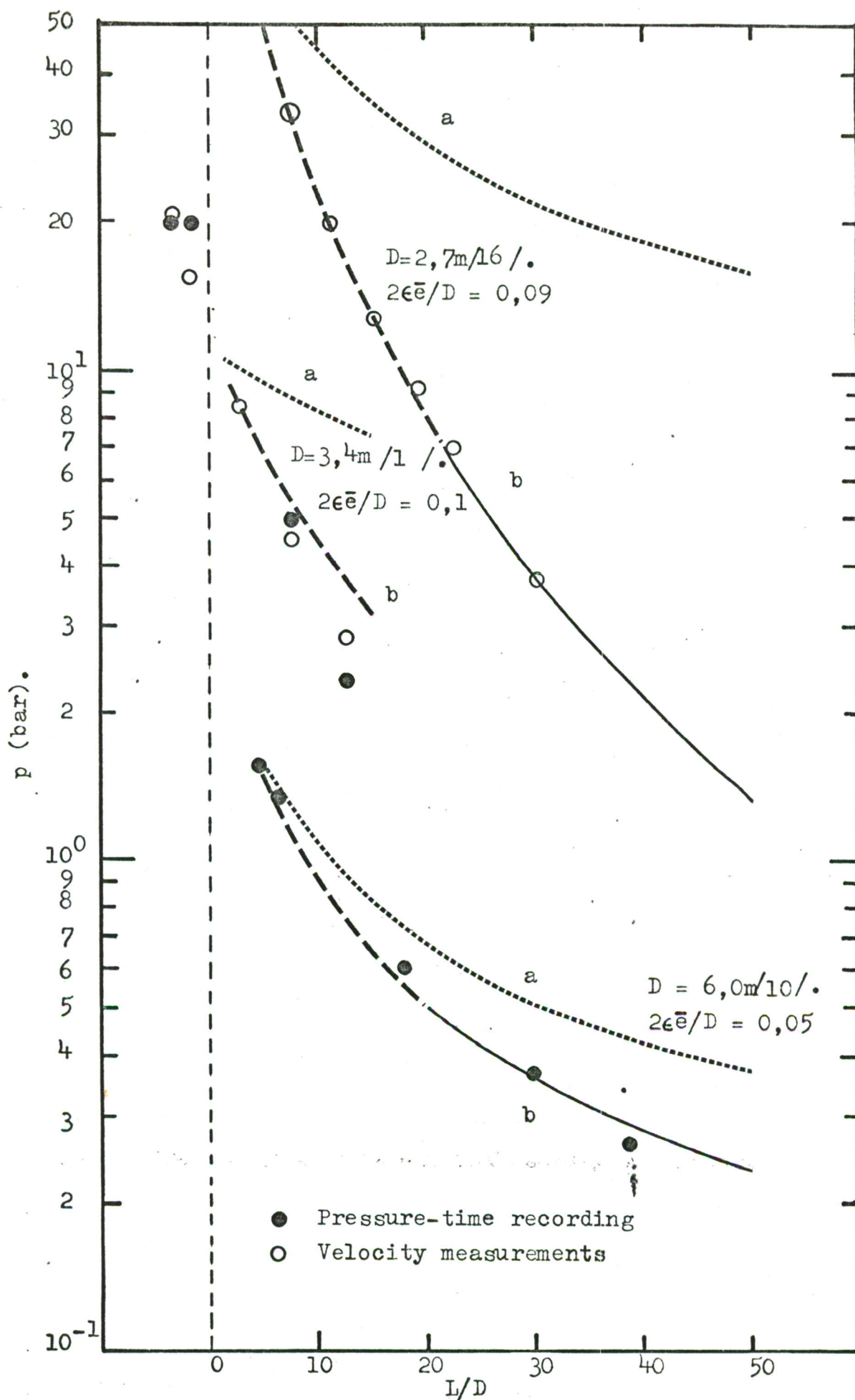


Fig.3.2e The same data as in Fig.3.2d except for using pressures explicitly.



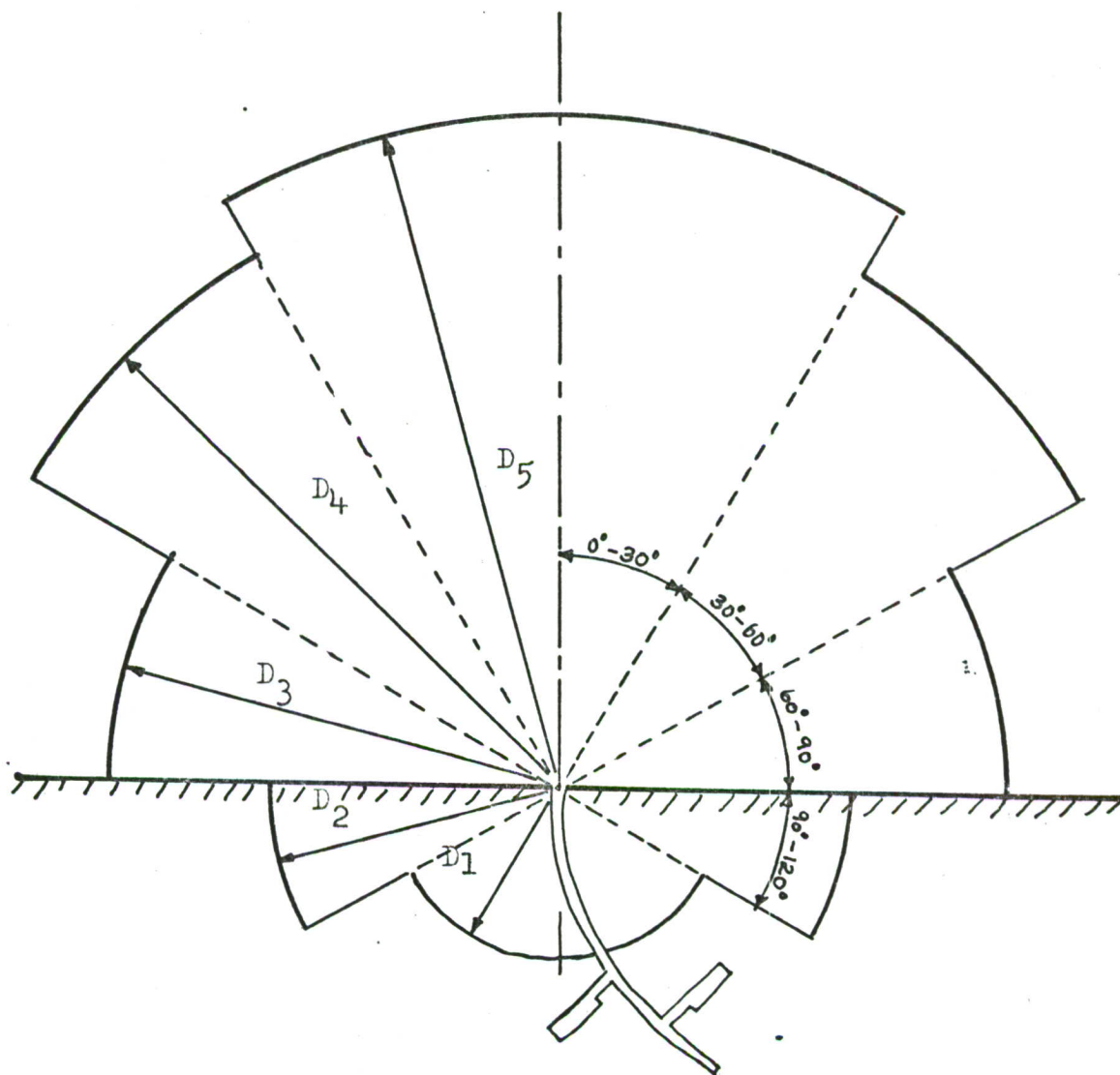
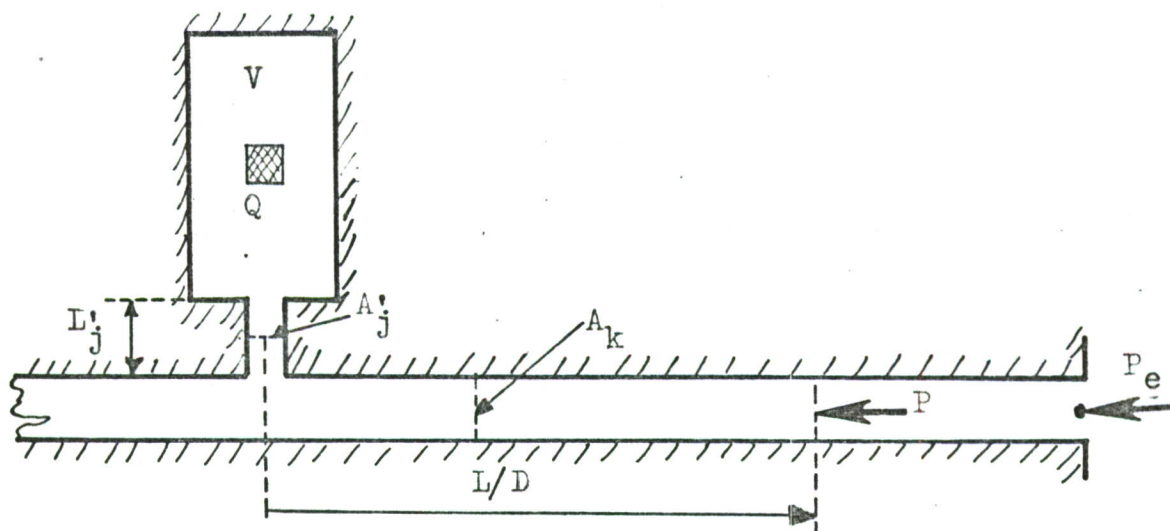


Fig.4.a The definition of external safety distances.



$V$  = 1760 m<sup>3</sup>, storage chamber volume

$A'_j$  = 10 m<sup>2</sup>, branch passageway cross-sectional area

$A_k$  = 20 m<sup>2</sup>, main passageway cross-sectional area

$D$  = 5 m, effective diameter of main passageway

$L'_j$  = 10 m, length of branch passageway

$Q$  = 88000 kg TNT, Net Explosive Quantity

$Q/V$  = 50 kg/m<sup>3</sup>, loading density

$Q/V_t$  = effective loading density

$V_t$  =  $V + A'_j \cdot L'_j + 2 L A_k$  = total effective volume

$p$  = pressure at distance  $L/D$  from exit of branch passageway

$P_e$  = pressure at the exit

Fig. 4.b Definitions of terms used in the connected chamber storage site discussed in the text



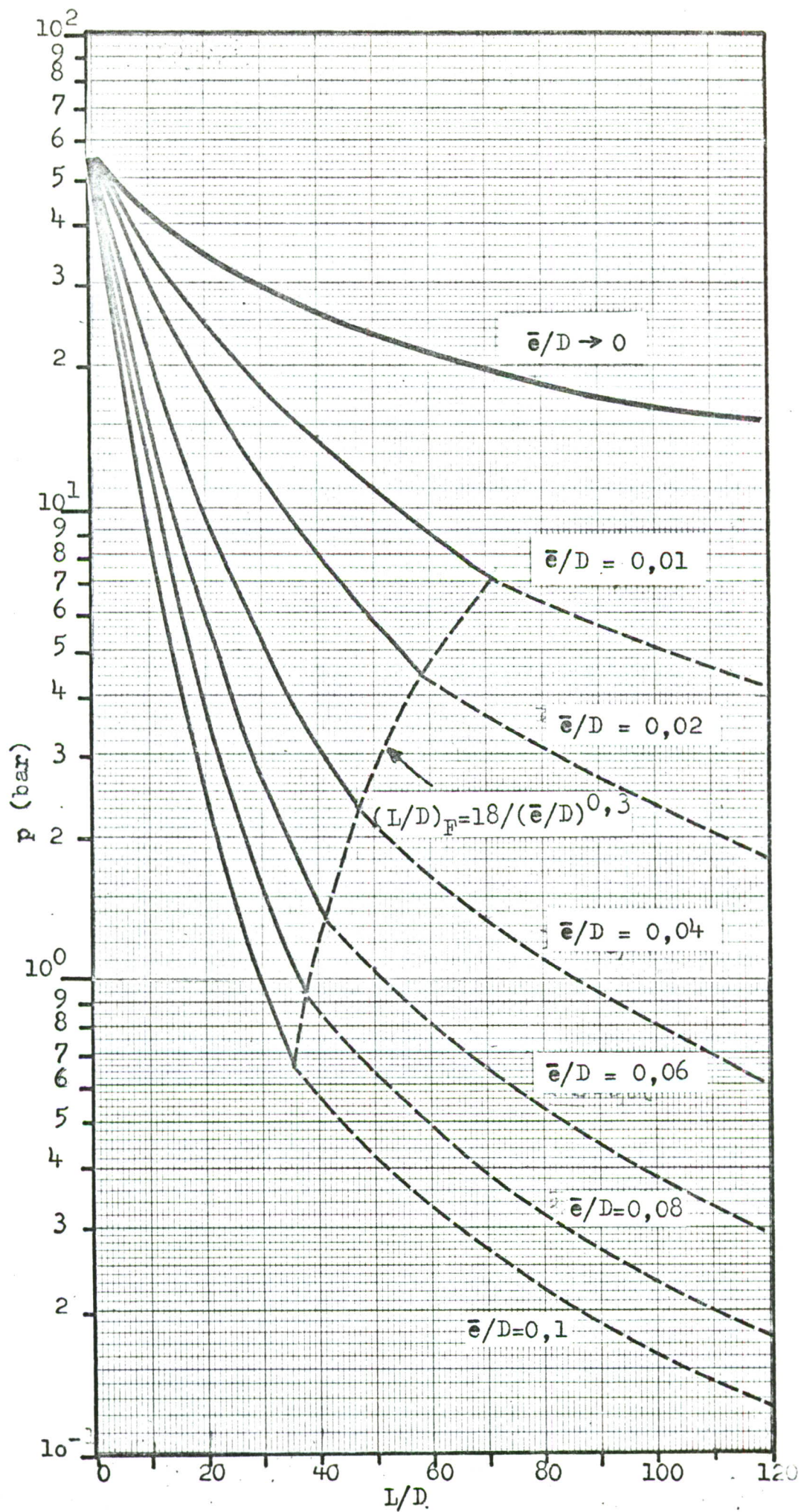


Fig.4.c Peak pressure versus distance in tunnel diameters for the connected chamber storage site discussed in the text with relative average wall roughness  $\bar{e}/D$  as parameter.



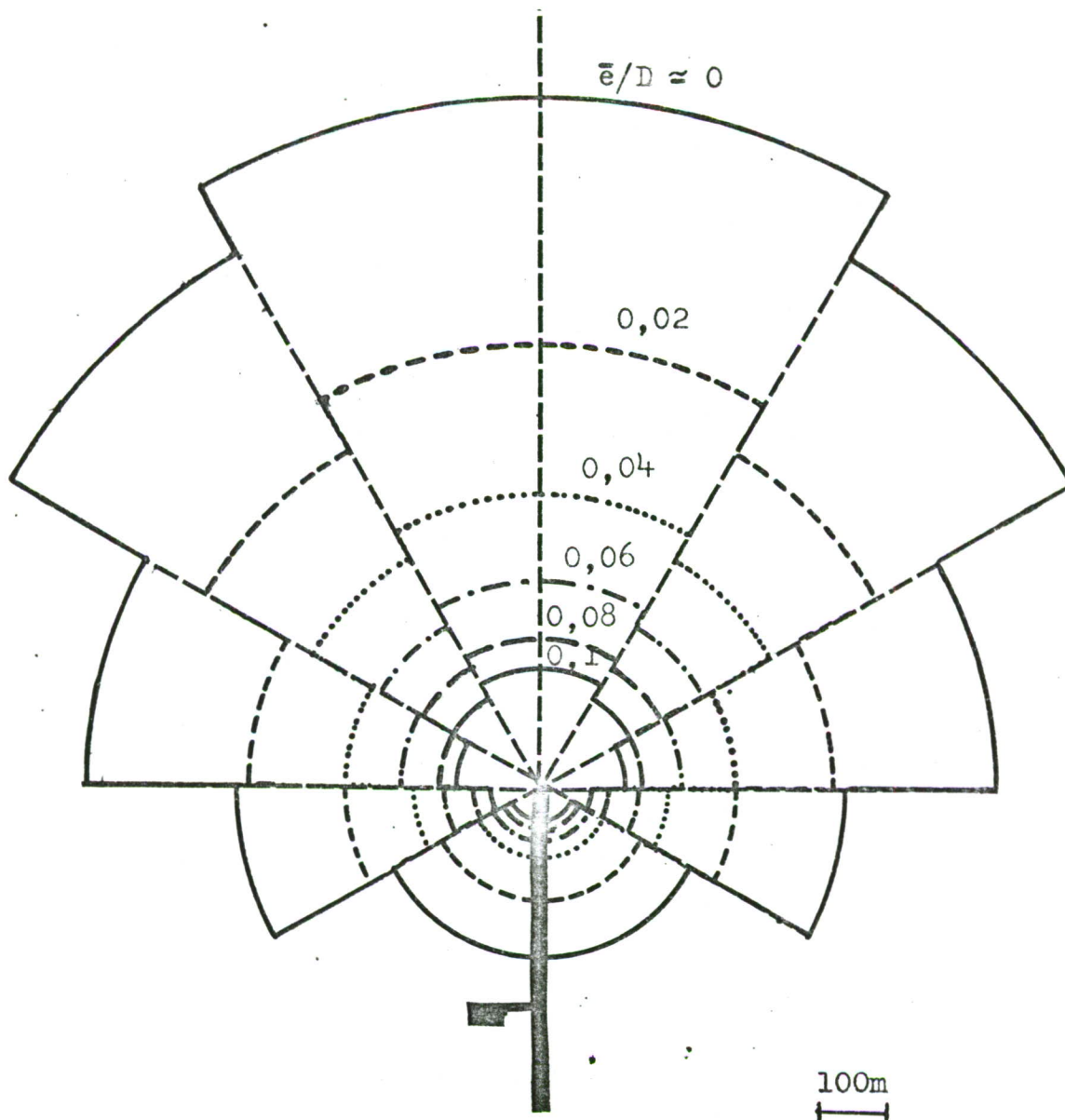


Fig.4.d Safety distances for an underground ammunition storage site with an essentially smooth-walled tunnel in comparison with tunnels having a relative wall roughness  $\bar{e}/D$  ranging from 0,02 to 0,1.